# On the Effects of Climate Policy Uncertainty

Facundo Luna

Rutgers University - New Brunswick *

September 24, 2025

**Abstract**

This paper identifies and quantifies the macroeconomic effects of a distinct form of economic risk: Climate Policy Uncertainty (CPU). Using monthly U.S. data (1985–2024) and news-based indices, I show that a one-standard-deviation shock reduces output and investment, raises unemployment, and lowers carbon emissions, suggesting a sectoral reallocation in the energy sector towards greener technologies. State-dependent impacts, even after controlling for standard measures of financial and economic policy uncertainty, shows that an exogenous shock to CPU is contractionary during economic expansions (reducing investment, output and emissions) but has no discernible effect during recessions. This asymmetric potency differs from the transmission of standard uncertainty shocks, which are contractionary in both states of the business cycle. To rationalize these findings, I develop a two-sector (green/brown) New Keynesian DSGE model with financial frictions and Epstein-Zin preferences. The model show that CPU shocks predominantly operate through an asset-quality channel (through brown-capital collateral, tightening credit, and prolonging downturns) rather than through carbon tax-volatility effects, emphasizing the role of financial frictions in shaping the macroeconomic and sectoral dynamics of the green transition. Climate policy is a source of macroeconomic volatility and shows that policy credibility is critical for a stable transition.

*rl870@economics.rutgers.edu

# 1 Introduction

Climate change presents not only environmental and social challenges but also growing macroeconomic and financial risks. In response, governments around the world are adopting or considering ambitious climate policies aimed at reducing greenhouse gas emissions and steering economies toward sustainable development. However, the pace, scope, and credibility of these policies remain highly uncertain. This uncertainty, referred to as Climate Policy Uncertainty (CPU hereafter), has emerged as a salient and potentially destabilizing force that can affect firm behavior, investment decisions, asset prices, and macroeconomic dynamics more broadly. This climate policy uncertainty tends to lower aggregate investment and output, but has asymmetric impacts across sectors (NGFS, 2024).

Climate Policy Uncertainty (CPU) refers to the ambiguity surrounding the future path, implementation details, stringency, timing, and economic consequences of policies aimed at mitigating climate change or adapting to its impacts (NGFS, 2024). While a single, universally adopted definition remains elusive, the core concept revolves around the lack of clarity that economic agents face when forming expectations about the policy landscape relevant to climate issues (Philip, 2024). This uncertainty can stem from various sources, including debates over the introduction or level of carbon taxes (Monasterolo et al., 2024), the design of subsidies for renewable energy, the scope and enforcement of environmental regulations, the outcomes of international climate negotiations, potential legal challenges to enacted policies, and the influence of political cycles or elections on policy continuity (Philip, 2024). It also considers uncertainty arising from delays in implementing announced policies or the credibility between long-term climate targets and near-term policy actions. Furthermore, uncertainty about future technological advancements in green or abatement technologies can interact with policy uncertainty, complicating investment decisions (Ferriani et al., 2024).

Recent empirical work highlights the economic relevance of CPU, showing that periods of amplified uncertainty about climate regulations are associated with increased volatility in financial markets and reduced investment in carbon-intensive sectors. However, the macroeconomic transmission mechanisms of CPU remain insufficiently understood, and its short to medium-run effects on key economic aggregates, such as output, inflation, employment, and credit flows, are still un-

derexplored. Moreover, the theoretical reinforcements that could explain the empirical patterns observed in the data have not yet been fully integrated into mainstream macroeconomic models.

This paper investigates the macroeconomic and financial fallout of Climate Policy Uncertainty (CPU) through a two-pronged empirical strategy. First, I trace the dynamic effects of a one-standard-deviation CPU shock on a broad set of real and financial indicators—GDP, inflation, investment, employment, equity prices, credit spreads, and even carbon emissions—by estimating local projections à la Jordà (2005) with monthly, news-based CPU indices for the U.S. (Baker et al., 2019; Palikhe et al., 2024). This nonparametric framework lets the data speak flexibly about impulse responses, uncovering that, in an unconditional setting, CPU shocks are contractionary in magnitude and duration, much like VIX or EPU shocks, but with the added effect of reallocating output from high-carbon toward green energy sectors.

Building on this, I split the sample by business-cycle phase to estimate state-dependent responses in the spirit of Ramey and Zubairy (2018). The results reveal a distinctive CPU signature: during expansions, shocks sharply depress investment, output, and emissions, yet in recessions their effects disappear. This asymmetry stands in contrast to conventional uncertainty shocks—which dampen activity regardless of cyclical slack—and points to a unique transmission channel for CPU that depends critically on the economy's underlying capacity.

Second, I rationalize the empirical findings within a structural general equilibrium framework. I develop a two-sector New Keynesian dynamic stochastic general equilibrium (DSGE) model with green and brown production sectors, financial frictions à la Gertler and Karadi (2011), nominal rigidities à la Rotemberg (1982), and environmental externalities (Heutel, 2012). Households feature recursive Epstein–Zin preferences, allowing for a rich intertemporal risk structure and long-run environmental valuation. Climate policy uncertainty enters the model in two different ways: a stochastic process affecting the expected future relative taxation of emissions in the brown sector or as a process of capital quality volatility in the brown sector, thereby influencing capital allocation, firm valuation, and financial intermediation. The transmission works through three margins: precautionary savings, sectoral capital reallocation, and the amplification supplied by leveraged intermediaries whose balance sheets are exposed to brown collateral values.

The parameters of the stochastic-volatility processes are chosen so that the model's simulated impulse response functions and the associated second moments closely replicate their empirical

counterparts. I show that the model with the CPU modeled as capital quality volatility can reproduce key empirical patterns observed in the local projection analysis, including contractionary effects on output and investment, as well as increased spreads in the financial sector. The theoretical framework further explains the mechanisms through which the CPU transmits to the real economy, highlighting the role of sectoral capital reallocation, precautionary savings behavior, and the amplification effects induced by financial frictions.

The remainder of this paper proceeds as follows. Section 2 surveys the relevant empirical and theoretical literature concerning climate policy uncertainty, establishing the context for our analysis. Section 3 details the data sources and outlines the econometric methodology employed for estimating empirical Impulse Response Functions (IRFs) using Local Projections. Subsequently, Section 4 presents the core empirical findings, reporting the estimated IRFs under a baseline specification and a state-dependent framework that accounts for the prevailing climate policy uncertainty regime. To interpret these empirical regularities, Section 5 develops and utilizes a theoretical Dynamic Stochastic General Equilibrium (DSGE) model to understand the underlying transmission mechanisms, and section 6 presents the mains results from the quantitative model. Section 7 concludes by summarizing the key findings and discuss policy implications.

## 2 Literature Review

Uncertainty has long been recognized as a fundamental driver of macroeconomic fluctuations. Early theoretical contributions by Bernanke (1983) and (Pindyck, 1986) formalized the idea that high uncertainty creates "real options" for firms, inducing them to delay irreversible investment until future conditions become clearer. Building on this intuition, more recent studies emphasize that uncertainty shocks operate through multiple channels. Gilchrist, Sim, and Zakrajšek (2014) show that financial frictions amplify the effects of uncertainty by widening credit spreads and tightening external finance constraints. Basu and Bundick (2017) highlights demand-side channels, demonstrating that uncertainty shocks reduce output, investment, and employment under nominal rigidities, with monetary policy cushioning their impact except at the zero lower bound.Bloom et al. (2018) further document that recessions are marked by both adverse first-moment and second-moment shocks, with uncertainty itself depressing productivity growth by

stalling firm-level reallocation. Together, this body of work underscores that uncertainty shocks can be contractionary, but their transmission depends critically on financial conditions, price stickiness, and the state of the business cycle.

A second strand of research has focused on uncertainty related specifically to government policy. Baker et al. (2016) pioneered the development of the Economic Policy Uncertainty (EPU) index, a newspaper-based measure of uncertainty over the economic policy environment. Their work shows that spikes in policy uncertainty are associated with reductions in investment and employment, increased volatility in the stock market, and a higher probability of recessions. Subsequent contributions extend this methodology to sector-specific domains, including trade policy (Caldara et al., 2020) and geopolitical risks (Caldara and Iacoviello, 2022), finding that uncertainty about the policy environment can depress investment and alter international capital flows. These results highlight that not all uncertainty is alike: when embedded in government action, it operates through both expectations about regulation and financial market perceptions of risk.

Building on these insights, a rapidly growing literature examines environmental and climate policy uncertainty (hereafter CPU) as a distinct form of policy risk. This research emphasizes that the credibility, timing, and enforcement of environmental regulations are highly volatile, creating uncertainty that directly affects both the "brown" and "green" sectors of the economy. Palikhe et al. (2024) develops a large-scale newspaper-based Environmental Policy Uncertainty (EnvPU) index for the United States, showing that increases in EnvPU reduce investment and employment in environmentally regulated industries and that political cycles shape the magnitude of these effects. Noailly et al. (2022) constructs a machine-learning-based EnvPU index, demonstrating that higher uncertainty lowers the probability that clean technology startups secure venture capital funding and increases the stock volatility of green firms. Extending this work, Noailly et al. (2024) build a granular Environmental and Climate Policy (EnvP) index that captures the volume, sentiment, and topical composition of environmental news, showing that increased policy salience supports clean investment while weighing on brown-sector returns. Beyond the U.S., Berestycki et al. (2022) find that CPU reduces investment in pollution-intensive sectors across OECD countries, while Philip (2024) documents that Swedish CPU shocks widen green bond spreads, raising financing costs for low-carbon transitions.Gavriilidis (2021) shows that spikes in U.S. CPU, linked to policy debates and failed legislation, coincide with declines in $CO_2$ emissions, suggesting re-

allocation from carbon-intensive to greener production. At the firm level, Ren et al. (2022) report that CPU reduces productivity in Chinese firms by constraining R&D and cash flow. Collectively, these studies converge on the view that CPU shapes sectoral investment decisions, reallocating resources between high- and low-carbon activities, and increases financing costs for firms exposed to regulation. Yet, while this literature highlights sectoral and firm-level reallocations, it pays less attention to the financial system as a transmission channel. When the collateral value of brown capital becomes uncertain, the effects of CPU are not confined to regulated industries but spill over into aggregate credit supply and macroeconomic activity, a gap this paper seeks to address.

This paper contributes to and extends each of these strands of literature. First, in relation to the broader uncertainty literature (Bernanke, 1983; Pindyck, 1986; Gilchrist et al., 2014; Basu and Bundick, 2017; Bloom, 2009; Bloom et al., 2018), I show that climate policy uncertainty has state-dependent effects: unlike standard uncertainty shocks, CPU is contractionary during expansions but has muted effects during recessions, highlighting that its transmission differs fundamentally from generic uncertainty. Second, relative to the economic policy uncertainty literature (Baker et al., 2016, 2019; Caldara et al., 2020; Caldara and Iacoviello, 2022), I construct a composite CPU index that combines both regulatory and financial-market-based dimensions, showing that CPU shocks propagate not only through expectations but also through the financial system.

Next, relative to the emerging environmental and climate policy uncertainty literature (Palikhe et al., 2024; Noailly et al., 2022, 2024; Berestycki et al., 2022; Philip, 2024), I go beyond documenting sectoral reallocations and financing constraints by showing that CPU shocks transmit primarily through financial frictions. Specifically, uncertainty surrounding climate regulation reduces the perceived collateral value of carbon-intensive (brown) capital, tightening credit conditions, and amplifying downturns. This mechanism generates an economy-wide contraction, not just a reallocation across sectors, because banks and intermediaries shorten lending when the quality of brown assets as collateral becomes uncertain. Modeling CPU as a capital-quality volatility shock, therefore, captures the financial amplification channel more accurately than treating it as pure carbon-tax volatility shock. While carbon-tax volatility can explain sectoral shifts between green and brown investment, it lacks the capacity to reproduce the observed aggregate contractionary effects. In contrast, the capital quality channel aligns both with empirical impulse responses and with the theoretical literature that stresses the vulnerability of financial systems to the devaluation

of carbon-intensive assets.

Finally, on the theoretical front, my DSGE framework advances existing models (Fried et al., 2021; Khalil and Strobel, 2023; Huang and Punzi, 2024) by explicitly distinguishing between carbon-tax volatility shocks and brown-capital quality shocks, and by incorporating Epstein–Zin preferences to capture precautionary behavior and long-run environmental valuation. By linking these empirical and theoretical contributions, the paper provides a unified framework for understanding CPU as both a macroeconomic and a financial stability risk.

# 3 Data and Methodology

## 3.1 Data

This paper uses monthly U.S. macroeconomic and financial data spanning 1985-01 to 2021-12 from the Federal Reserve Economic Data (FRED) database maintained by the Federal Reserve Bank of St. Louis. The set of variables includes industrial production (INDPRO), the personal consumption expenditure index (PCEPI) as a measure of inflation, the effective federal funds rate (FEDFUNDS), credit to nonfinancial firms (BUSLOANSNF), the unemployment rate (UNRATE), Gross Fixed Capital Formation as a proxy from investments, and personal consumption expenditures (PCE). In addition, I include a measure of U.S. $CO_2$ emissions to capture the environmental response.

To capture climate and environmental policy uncertainty, I use two independent news-based indices. The first is the Environmental Policy Uncertainty (EnvPU) index compiled by Palikhe et al. (2024). This index measures uncertainty surrounding U.S. environmental regulation using a text-based approach applied to over 300 million newspaper articles from 1985 to 2019. The index identifies articles that simultaneously reference economic or policy-related terms, general uncertainty keywords, and a curated list of 31 environment-specific terms such as "carbon tax" or "EPA regulation." The monthly count of such articles is normalized to create a time-series index that reflects perceived regulatory uncertainty. This method builds on the framework of Baker et al. (2016) but is tailored to the environmental policy context. The authors show that the index correlates with major regulatory events and has predictive power for firm-level investment and employment responses, particularly in pollution-intensive sectors.

Secomd, I use the "Equity Market Volatility Tracker: Energy and Environmental Regulation" index (VIX-EER), which is a specialized index developed by Baker et al. (2019) [1]. It measures the extent to which equity market volatility is associated with news related to energy and environmental regulation. This tracker is part of a broader set of indices that analyze how different policy areas influence market volatility. The EMV Tracker counts monthly articles from 11 major U.S. newspapers (e.g., New York Times, Wall Street Journal, Chicago Tribune) that contain terms relate to **E**conomy, **M**arket and **V**olatility. The raw counts of EMV articles are scaled by the total number of articles in the same newspaper and month to account for varying news volumes. The resulting series is multiplicatively rescaled to match the mean value of the CBOE Volatility Index (VIX), ensuring the EMV Tracker moves with the VIX and the realized volatility of S&P 500 returns.

Finally, to capture a unified measure of climate and environmental policy uncertainty, I construct a composite index by combining the Environmental Policy Uncertainty (EnvPU) index and the Equity Market Volatility Tracker for Energy and Environmental Regulation (VIX-EER). Both indices are derived from text-based analysis of major U.S. newspapers, with EnvPU focusing on regulatory uncertainty related to environmental issues and VIX-EER capturing volatility in equity markets linked to energy and environmental policy news. Using principal component analysis (PCA), I extract the first principal component from these two series, which represents the largest shared variation and effectively summarizes their common informational content. This composite index serves as a more comprehensive proxy for climate policy uncertainty, reflecting both regulatory and market-based dimensions.

### 3.2 Methodology

To estimate the dynamic effects of climate and environmental policy uncertainty on key macroeconomic and financial variables, I employ the local projection (LP) method proposed by Jordà (2005). Local projections offer distinct advantages over vector autoregressions (VARs) in this context. Unlike VARs, which require accurate specification of the joint dynamics of all variables, LPs estimate impulse response functions (IRFs) horizon by horizon, imposing minimal assumptions about the underlying data-generating process (DGP). This makes LPs more robust to misspecification, particularly when structural breaks or complex dynamics—common in uncertainty

[1] Available at https://fred.stlouisfed.org/series/EMVENRGYENVREG/

shocks—are present (Ramey, 2018; Plagborg-Møller and Wolf, 2021). Additionally, LPs facilitate flexible extensions, such as state-dependent or nonlinear models, which are well-suited to capture potential asymmetries in responses to climate policy uncertainty (Tenreyro and Thwaites, 2016; Barnichon and Brownlees, 2019).

The LP framework estimates IRFs by regressing the future value of an outcome variable on a climate policy uncertainty (CPU) shock and a set of controls. For each horizon $h = 0, 1, \ldots, 60$, I estimate the following equation:

$$y_{t+h} = \alpha_h + \beta_h \cdot \text{CPU Shock}_t + \sum_{\tau=1}^{p} \phi_{\tau,h} y_{t-\tau} + \sum_{\tau=1}^{p} \sigma_{\tau,h} \text{CPU}_{t-\tau} + \sum_{\tau=1}^{p} \lambda_{\tau,h} Z_{t-\tau} + \varepsilon_{t+h}, \tag{1}$$

where $y_{t+h}$ represents the different macroeconomic or financial variables (e.g., industrial production, investment, emissions, S&P 500 index) at time $t + h$, and $\text{CPU Shock}_t$ is the standardized shock for each CPU index at time $t$. The coefficient $\beta_h$ represents the IRF at horizon $h$ to a one-standard-deviation CPU shock. The vector $Z_t$ includes lags of control variables, specifically the U.S. Economic Policy Uncertainty index (Baker et al., 2016) and the VIX index, to isolate CPU effects from broader economic and financial uncertainty. The number of lags $p$ is selected using the Akaike Information Criterion (AIC) based on an auxiliary VAR, ensuring robust control for the DGP's dynamics (Olea et al., 2025). Standard errors are corrected for heteroskedasticity using robust estimators, and IRFs are reported in percent deviations from baseline with 90% confidence intervals.

As a robustness check, I also estimate an instrumental variable (IV) LP model

$$y_{t+h} = \alpha_h + \beta_h \cdot \text{CPU}_t + \sum_{\tau=1}^{p} \phi_{\tau,h} y_{t-\tau} + \sum_{\tau=1}^{p} \lambda_{\tau,h} Z_{t-\tau} + \varepsilon_{t+h}, \tag{2}$$

where $\text{CPU}_t$ is instrumented by $\text{CPU Shock}_t$. The IV approach ensures that the estimated IRFs capture the causal effect of exogenous CPU innovations, controlling for feedback from macroeconomic conditions (Olea et al., 2025).

The CPU shock is constructed to isolate exogenous innovations in policy uncertainty, following standard practices in the uncertainty literature (Jurado et al., 2015). The CPU indices are news-based measures derived from the frequency of articles in major U.S. newspapers referencing cli-

mate policy and uncertainty. To extract unanticipated shocks, I estimate an autoregressive model with data-driven lag selection:

$$\text{CPU}_t = \alpha + \sum_{\tau=1}^{p} \phi_\tau \text{CPU}_{t-\tau} + \sum_{\tau=1}^{p} \gamma_\tau W_{t-\tau} + \varepsilon_t^{\text{CPU}}, \tag{3}$$

where $W_t$ includes lagged macroeconomic controls (e.g., personal consumption expenditures, unemployment rate, core inflation, investment, industrial production, S&P 500, business loans, federal funds rate) in levels or first differences based on stationarity tests (Dickey-Fuller). The lag length $p$ is selected via AIC from an auxiliary VAR, ensuring all relevant dynamics are captured (Olea et al., 2025). The residuals $\varepsilon_t^{\text{CPU}}$ represent the unexpected component of CPU. The standardized shock is:

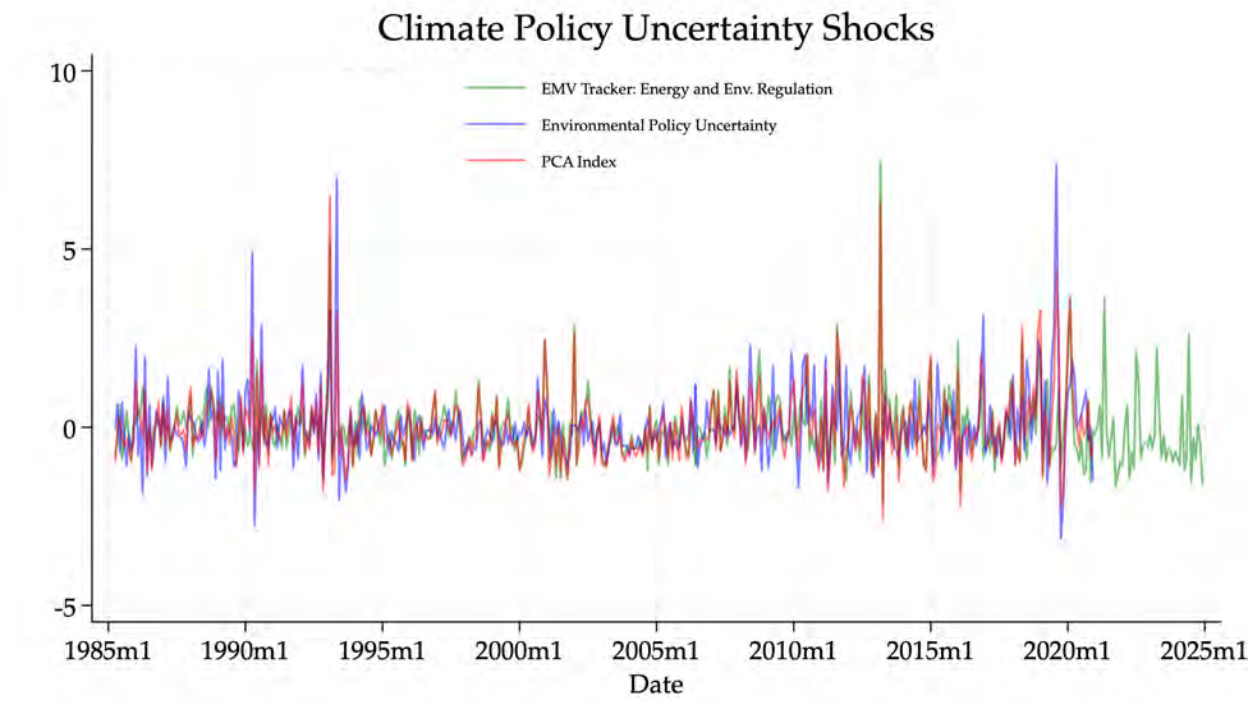
$$\text{Shock}_t = \frac{\varepsilon_t^{\text{CPU}}}{\hat{\sigma}_\varepsilon}, \tag{4}$$

where $\hat{\sigma}_\varepsilon$ is the sample standard deviation of the residuals. This normalization ensures comparability across indices and consistency with model-based IRFs, capturing a one-standard-deviation shock.

The resulting shock series (figure 1) displays distinct spikes that align with major environmental policy events, reflecting heightened periods of perceived regulatory uncertainty. Notable peaks correspond to the 1986 renewal of the Clean Water Act, the first official Earth Day in 1990, and the 1993 proposal of the BTU tax. A significant increase in uncertainty is also observed around the transition to the George W. Bush administration in January 2001, which marked a shift in climate policy direction, including the rejection of the Kyoto Protocol as "not acceptable" to the administration or Congress. Additional spikes occur during the 2010 BP oil spill and the 2011 rollback of air quality standards. The EMV Tracker, in particular, registers a prominent rise in mid-2015, coinciding with the announcement of the Clean Power Plan, which introduced the first nationwide carbon emission standards for existing power plants, and the legislative extension and phase-down of renewable energy tax credits later that year. These episodes illustrate moments of policy redefinition and increased regulatory ambiguity. In contrast, the indices do not show substantial responses to international agreements with limited domestic enforcement, such as the 2015 adoption and the 2017 U.S. withdrawal from the Paris Agreement, which lacked Congressional

ratification and had little immediate impact on U.S. policy.

**Figure 1:** Standardized CPU shock series.




Then, to examine whether CPU shocks propagate differently in expansions versus recessions, I extend the LP framework to incorporate state dependence, following Ramey and Zubairy (2018). The state-dependent LP model is:

$$\begin{aligned} y_{t+h} = I_{t-1} \left[ \alpha_h^H + \beta_h^H \text{Shock}_t + \sum_{\tau=1}^{p} \phi_{\tau,h}^H y_{t-\tau} + \sum_{\tau=1}^{p} \lambda_{\tau,h}^H Z_{t-\tau} \right] + \\ (1 - I_{t-1}) \left[ \alpha_h^L + \beta_h^L \text{Shock}_t + \sum_{\tau=1}^{p} \phi_{\tau,h}^L y_{t-\tau} + \sum_{\tau=1}^{p} \lambda_{\tau,h}^L Z_{t-\tau} \right] + \varepsilon_{t+h} \end{aligned} \tag{5}$$

Where $I_{t-1}$ is a dummy variable indicating the state of the economy (e.g., expansion vs recession) at the time of the shock, $Z_{t-1}$ is a vector of control variables, and the coefficients $\beta_{A,h}$ and $\beta_{B,h}$ trace the impulse response in each respective state. This state is determined by an observable macroeconomic variable, such as whether the unemployment rate is above a certain threshold. For the baseline scenario, I use the sample median of 5.7% for my periods, while in Appendix A.4,

I present the Impule Response Functions for different cutoffs.

The vector $Z_{t-1}$ includes the same set of control variables as the linear model—lags of the VIX and the EPU indices, to ensure that the estimated responses are not driven by other forms of uncertainty. By estimating this equation for each horizon h from 0 to 60 months, we can construct and compare the full impulse response functions for each state, providing a robust test of whether the effects of CPU are contingent on the business cycle.

Additionally, in Appendix A.5 we perform a robustness test of the state-dependent methodology stated in Auerbach and Gorodnichenko (2012):

$$y_{t+h} = \alpha_h + \beta_h^L \cdot F(\mathcal{S}_{t-1}) \cdot \text{Shock}_t + \beta_h^H \cdot \big(1 - F(\mathcal{S}_{t-1})\big) \cdot \text{Shock}_t + \sum_{\tau=1}^{p} \phi_{\tau,h} y_{t-\tau} + \sum_{\tau=1}^{p} \lambda_{\tau,h} Z_{t-\tau} + \varepsilon_{t+h}, \quad (6)$$

where $\beta_h^L$ and $\beta_h^H$ are the IRFs in low- and high-uncertainty regimes, respectively. The transition function $F(\mathcal{S}_t)$, which weights the high unemplomentregime, is:

$$F(\mathcal{S}_t) = \frac{\exp\big(-\gamma(\mathcal{S}_t - \bar{\mathcal{S}})\big)}{1 + \exp\big(-\gamma(\mathcal{S}_t - \bar{\mathcal{S}})\big)}, \quad (7)$$

Here $\mathcal{S}_t$ denotes the unemployment rate with 6 periods moving average mean (mean $\bar{\mathcal{S}}$, normalized to unit variance so that $\gamma$ is scale-invariant), and $\gamma$ governs the smoothness of the regime transition (robustness checks with $\gamma \in \{1, 1.5, 2\}$ appear in Appendix A.5). Under this specification, $F(\mathcal{S}_t) \approx 1$ corresponds to recessionary periods, while $F(\mathcal{S}_t) \approx 0$ indicates expansions. The smooth-transition function thus flexibly captures nonlinear, state-dependent macroeconomic dynamics, consistent with the literature on regime-specific effects (Auerbach and Gorodnichenko, 2012). To avoid contemporaneous feedbacks from policy actions into whether the economy is in a recession or an expansion, we use the lagged indicator for $\mathcal{S}_t$.

## 4 Empirical Evidence

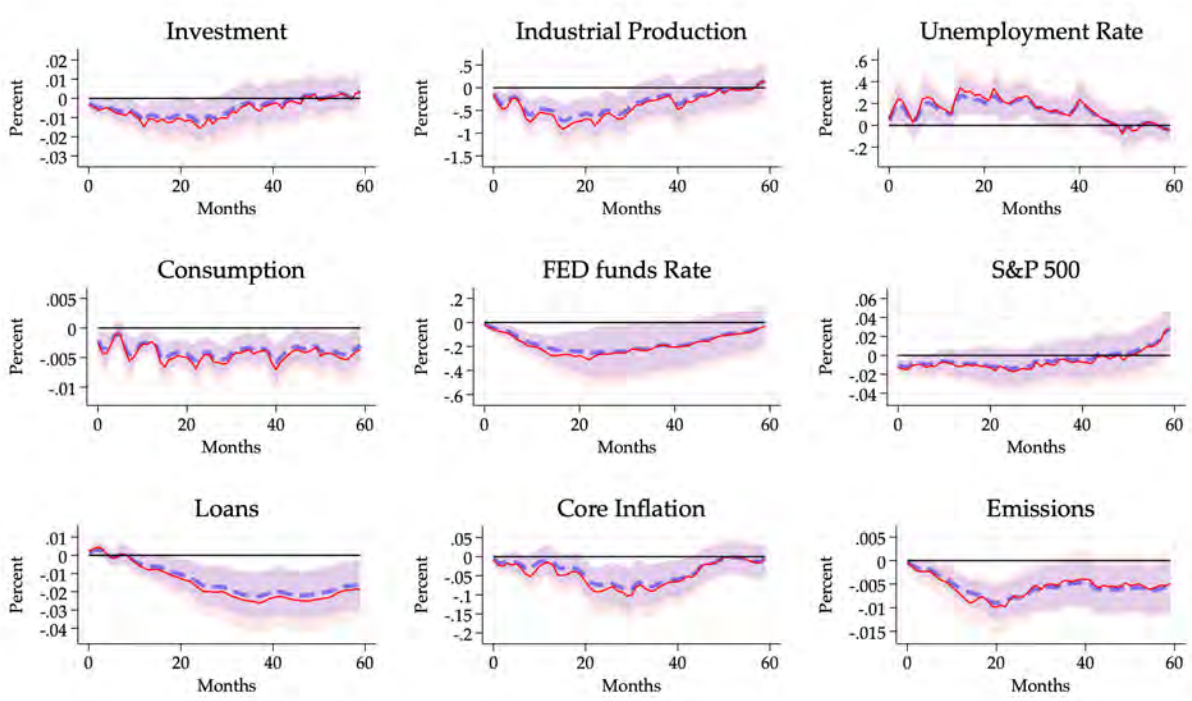
This section presents key macroeconomic and financial variables' impulse response functions (IRFs) to a standardized innovation in climate and environmental policy uncertainty. The shocks are derived from two indices: the Environmental Policy Uncertainty (EnvPU) index, and the Equity Market Volatility Tracker: Energy and Environmental Regulation, and the first component of

a PCA between both indices. I estimate impulse response functions (IRFs) using local projections over a 60-month horizon, with all specifications controlling for lags of the VIX, EPU indices and changes in the WTI oil prices to ensure we are identifying the marginal impact of the CPU shock. To isolate the unique impact of the CPU shock, we benchmark its effects against two established measures of uncertainty: the general U.S. Economic Policy Uncertainty (EPU, Baker et al. (2016)) and the VIX index as a proxy for aggregate financial uncertainty (Appendix A.3).

In this section, we present the Impulse Response Function from the PCA Index since this is a more comprehensive proxy for climate policy uncertainty, reflecting both regulatory and market-based dimensions, while in Appendix A.2, we present the IRF for the individual Indices as a robustness check.

Figure 2 illustrates the dynamic effects of a one–standard-deviation innovation in our composite climate-policy-uncertainty index, constructed via PCA from EnvPU and EMV-EER. Both the OLS-based (blue) and IV-based (red) estimates closely coincide, confirming that instrumenting the PCA index does not materially change the results. Taken together, these responses reveal a coherent story of how heightened climate-policy uncertainty propagates through the real economy and financial markets, consistent with the "negative-demand" mechanism emphasized by Baker et al. (2016) and the bank-lending amplification highlighted by Basu and Bundick (2017).

**Figure 2:** Impulse Response Functions to 1 sd PCA shock - OLS (blue) and IV (red)




Note: 90% CI - In OLS I use the Index shock while in the IV the shock instrument the index

The results point to a clear contractionary effect of CPU on the U.S. economy. Investment falls by about 1.5% on impact and remains persistently depressed for up to five years, while industrial production contracts by around 1%. Consistent with these contractions on the real side, the unemployment rate increases by 1 to 1.5 percentage points, while household consumption also declines, mirroring the response to investment. Together, these results highlight that CPU shocks operate as negative demand disturbances with lasting effects on aggregate activity.

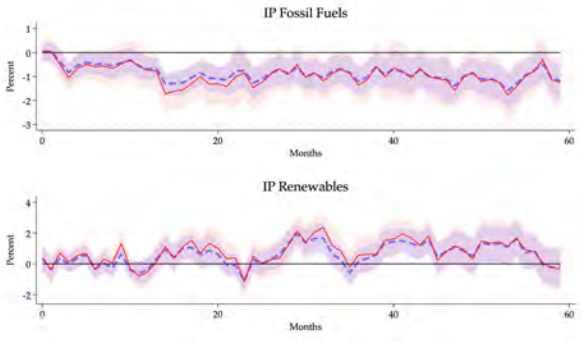
The financial side reveals an important amplification mechanism. Business loans contract sharply (around 2.5%), while equity valuations (S&P 500) fall, pointing to intensified financial stress. Since investment is particularly sensitive to financing conditions, the reduction in credit supply and asset valuations suggests that CPU shocks propagate through a tightening of financial frictions rather than simply delaying investment via a wait-and-see mechanism. This interpretation is reinforced by the monetary policy response: the federal funds rate declines persistently, consistent with the Federal Reserve counteracting the contractionary shock. Inflation also moderates, with core inflation falling by 0.5–1%, indicating that CPU shocks are disinflationary rather

than stagflationary.

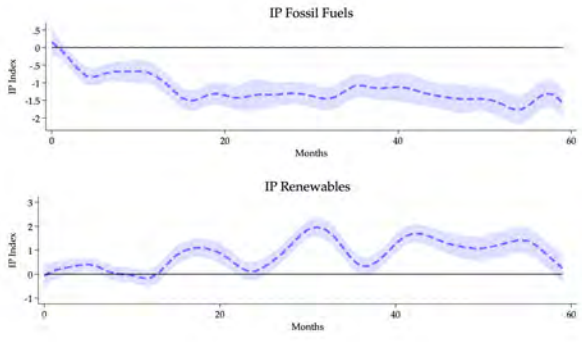
The crucial insights, however, come from comparing the CPU shock's signature to that of a VIX shock. While both are contractionary, two key differences emerge. First, the negative impact of a CPU shock on investment and industrial production appears more persistent than that of a VIX shock. Second, and most importantly, the shocks have starkly different environmental consequences. A VIX shock, representing a generic "risk-off" event, has no statistically significant impact on $CO_2$ emissions. In contrast, a CPU shock leads to an immediate and sustained drop in carbon emissions.

This divergence suggests that CPU is not just another measure of aggregate fear; it operates through a more targeted channel. To identify this channel, I turn to a sectoral analysis of the energy industry. Examining the left panel of Figure 3, and its smoothed LP analogue following Barnichon and Brownlees (2019), reveals that the fossil-fuel energy Industrial Production Index plunges about 1.5 points on impact (approximately 1.4% of its sample mean) and remains suppressed over the full 60-month horizon. By contrast, the overall Industrial Production Index (Figure 2) falls by at most one point at impact and rebounds more quickly. This more pronounced and enduring contraction in carbon-intensive output suggests that climate-policy uncertainty functions not merely as a broad demand shock but disproportionately penalizes fossil-fuel industries.

**Figure 3:** IP Index IRF to 1 sd PCA shock - Left OLS (blue) and IV (red) - OLS Right Smooth LP




Note: 90% CI




Note: 90% CI - OLS IRF to CPU shock

Regarding the renewable-energy IP index, it exhibits the inverse mirror image pattern: it remains flat or slightly negative in the first year, but then rebounds and grows positively by 1 to 2 points (1.3% to 2.6 % from the sample mean) between months 12 and 30, before slowly converging back toward zero. The post–one-year output gains in the renewable sector coincide with the

trough in fossil-fuel production, suggesting a reallocation toward cleaner energy sources.

Taken together with the behavior of total emissions, these sectoral responses point toward a structural shift rather than cyclical weakness. Whereas total industrial output and aggregate emissions both decline on impact under high uncertainty, emissions fall more steeply and remain lower for longer, tracking the fossil-fuel drop rather than the milder contraction of overall IP. Meanwhile, renewables expand, indicating that some of the cooling in aggregate industrial activity is offset by a sustained boost to clean-energy sectors. This differential behavior across fossil and renewable IP confirms that climate-policy uncertainty induces a compositional reallocation away from high-carbon electricity. This asymmetric response differs from the effects of VIX and EPU shocks, which are sector-neutral and have no differential impact on fossil fuel versus renewable energy production (see Appendix A.3).

These patterns are consistent with the mechanisms emphasized in Baker et al. (2016)and Basu and Bundick (2017). In their framework, uncertainty shocks weaken aggregate demand and tighten credit, but they also introduce precautionary incentives and alter relative returns across sectors. I see that here: fossil-fuel firms, facing ambiguous future regulations and financing constraints, cut back sharply. In contrast, renewable producers, whose long-term prospects look more stable under heightened regulatory risk for carbon, attract new investment and expand output. In short, the joint response for fossil and renewable IP supports the interpretation that climate-policy uncertainty not only depresses overall industrial activity but also favor a structural transition toward low-carbon electricity generation.

These findings reveal a multi-channel transmission of climate-policy uncertainty: it dampens investment and consumption, tightens financial conditions, and triggers an easing response from the central bank, all while permanently improving environmental outcomes through a lasting drop in fossil-fuel generation and a rise in renewables. Far from acting as a broad-based VIX-style shock, CPU operates as a targeted reallocation shock—specifically penalizing carbon-intensive industries and reshaping the composition of economic activity. Having established this channel, the next step is to ask under what macroeconomic conditions the sectoral reallocation effect is strongest, which I explore in the following state-dependent analysis.

### 4.1 State Dependent Impulse Response

The unconditional analysis established that Climate Policy Uncertainty (CPU) has a unique, sector-specific footprint. I now investigate the question motivated by this finding: under what macroeconomic conditions is this targeted reallocation channel most potent? To answer this, I estimate state-dependent impulse responses, separating the sample into two business-cycle regimes: expansions (low unemployment) and recessions (high unemployment). We define the recessionary state as periods where the unemployment rate is above its sample median (5.7%), in the spirit of Ramey and Zubairy (2018). To ensure our results are not sensitive to this particular threshold, Appendix A.4 reports robustness checks using alternative unemployment cut-offs as well as the identification approach of Auerbach and Gorodnichenko (2012).

Figure 4 presents a key empirical finding of this paper. The impact of a CPU shock is contingent on the state of the business cycle, demonstrating a clear asymmetry in its potency.

During Expansions (Low Unemployment), a CPU shock acts as a severe and disruptive contractionary force. It triggers a deep and statistically significant decline in investment, which falls by over 2% at its trough. This freeze in capital spending propagates quickly to the rest of the economy: industrial production contracts sharply, and the unemployment rate rises by approximately 0.4 percentage points. Financial conditions tighten in response, with bank lending falling for over two years. The Federal Reserve is forced to pursue a strong easing cycle, cutting the policy rate by nearly 50 basis points to counteract the negative demand shock.

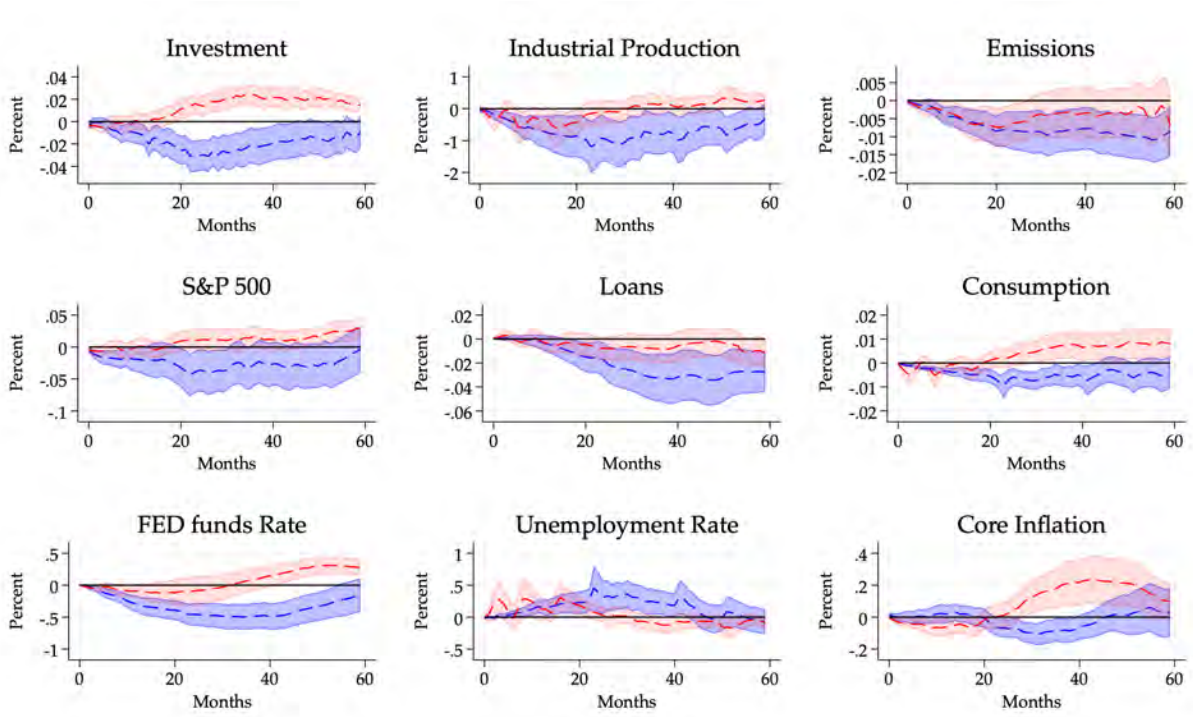
During Recessions (High Unemployment), the red lines illustrate a different reality. In periods when the economy is already weak, the same CPU shock is a non-event. The impulse responses for investment, stock market, lending, and unemployment are almost entirely flat and statistically indistinguishable from zero. There is a small drop in the first periods of the Industrial Production Index, which translate into a mild decrease in emissions for the first months, but is not sustained as in the expansion regime.

This asymmetric potency is a notable characteristic of CPU. While standard financial uncertainty, proxied by the VIX, is also more damaging in expansions, its effects in recessions are merely dampened, not eliminated (see Appendix A.4). The impact of CPU in recessions is not just weaker; it is zero. This suggests that the sectoral reallocation channel, which is the unique feature of CPU,

is effectively switched off when the economy is weak.

The economic intuition for this is tied to the "option to wait" (Bloom, 2009). In good times, firms are actively investing and expanding. Their primary constraint is uncertainty about the future, so a shock to the viability of carbon-intensive capital has a negative effect, causing them to postpone or cancel projects. In bad times, however, investment is already at a minimum. The binding constraints are weak demand and tight credit, not policy ambiguity. The sectoral reallocation channel becomes irrelevant because firms have no plans to invest in either the green or the brown sector. A shock to the relative attractiveness of capital types cannot influence a decision that is already on hold; the uncertainty shock is "pushing on a string."

**Figure 4:** State-Dependent IRFs to a 1 SD Shock in the Composite PCA Index

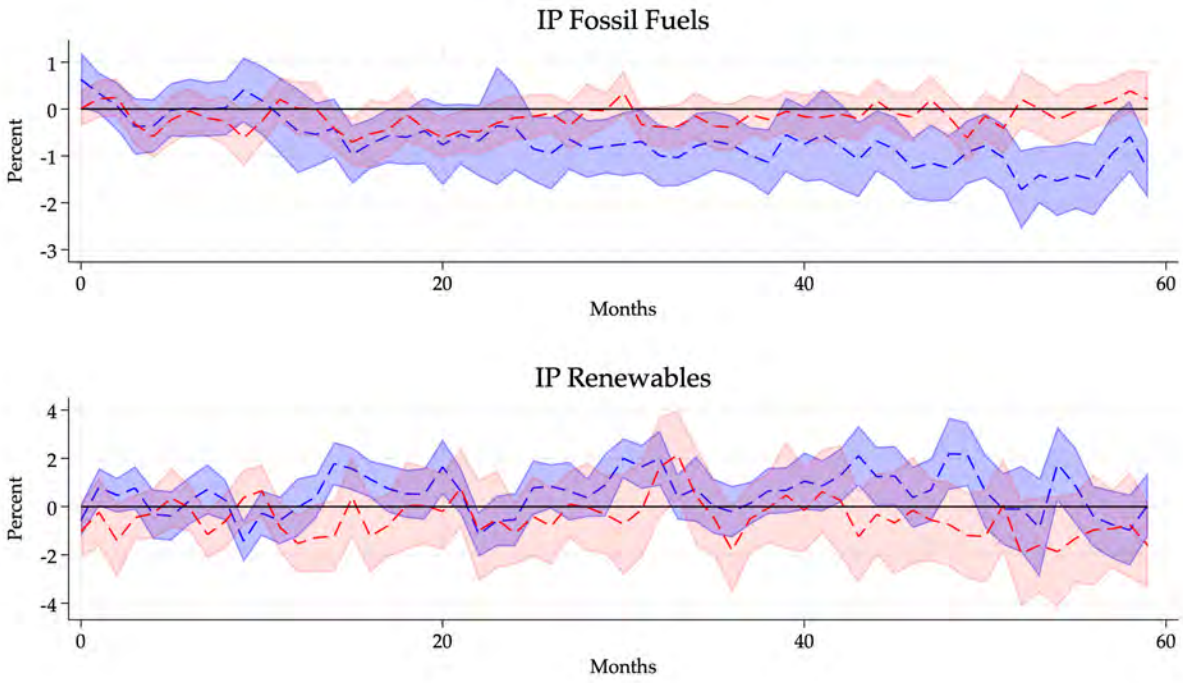



90% Confidence Bands. Red = High Unemployment; Blue = Low Unemployment.

The sectoral energy production data in Figure 5 provide direct and compelling evidence for this mechanism. In the expansionary state (blue), the CPU shock causes a collapse in fossil fuel production while leaving renewables unharmed. This is the sectoral reallocation channel in action: the shock's entire macroeconomic impact is driven by a targeted halt in carbon-intensive activity. In the recessionary state (red), however, the shock has no discernible impact on either

energy source. This confirms that the sectoral reallocation mechanism is the primary channel of transmission and that it is only operative during economic expansions.

**Figure 5:** State-Dependent IRFs for Fossil Fuel and Renewable Energy IP




Note: 90% CI. Blue = Low Unemployment (Expansion); Red = High Unemployment (Recession).

## 5 Model

The empirical evidence reveals that Climate Policy Uncertainty (CPU) is a distinct macroeconomic shock with a state-dependent footprint. Unlike standard measures of uncertainty, its potent contractionary effects are concentrated entirely in economic expansions, while it has no discernible impact during recessions. The underlying mechanism appears to be a powerful sectoral reallocation channel—a targeted disruption of carbon-intensive activity—that is only operative when the economy is strong.

To rationalize these specific empirical regularities, I develop a two-sector New Keynesian DSGE model explicitly designed to reproduce the asymmetric potency of CPU by capturing the sectoral and financial channels through which it propagates. It extends the work of Diluiso et al. (2021) and Ferrari and Nispi Landi (2024) by integrating several key, interconnected features. At

its core, the model features a two-sector (green/brown) production structure, which is essential for directly analyzing the sectoral reallocation between carbon-intensive and clean energy industries that the data points to as the primary transmission channel. We embed this sectoral core within a financial intermediation block with frictions à la Gertler and Karadi (2011), allowing us to capture the financial amplification of the shock, particularly how uncertainty about the future value of "brown" capital affects bank balance sheets, credit provision, and risk premia. Finally, the model features households with Epstein-Zin preferences. This preference structure is necessary for modeling a rational response to uncertainty itself, as it allows us to disentangle risk aversion from intertemporal substitution and to generate the precautionary savings and investment behavior that is central to the transmission of second-moment shocks (Basu and Bundick, 2017). Under EZ preferences, agents internalize the possibility of persistent adverse shocks, leading to stronger precautionary behavior and more pronounced adjustments in consumption, savings, and asset demand.

By integrating these features, the model provides a structural laboratory to test whether the empirically-observed dynamics can be explained by the interplay between sectoral reallocation and financial frictions under uncertainty. The following subsections present more details about the different sectors in this model in this context.

### 5.1 Households

The model considers a continuum of infinitely lived households with preferences over consumption and leisure. with Epstein-Zin recursive preferences (Epstein and Zin, 1991, 2013). This formulation addresses key limitations of the expected utility framework, as shown in Ackerman et al. (2013) and Hambel et al. (2021), who demonstrate that Epstein-Zin preferences yield markedly different and more robust policy implications in climate economics.

Each household consists of workers and bankers. Bankers operate financial intermediaries and transfer profits to the household, but cannot borrow from intermediaries owned by their own household. Workers supply labor and contribute their wages to the household. While individuals may switch occupations over time, the aggregate shares of workers and bankers remain constant.

The representative Household has a utility function over streams of consumption ($c_t$) and

leisure $(1 - L_t)$:

$$V_t = \left((1-\beta)\ \left(\left(c_t^{\omega}\ (1-L_t)^{1-\omega}\right)^{1-\rho}\right) + \beta\left[\mathbb{E}_t(V_{t+1}^{1-\sigma})\right]^{\frac{1-\rho}{1-\sigma}}\right)^{\frac{1}{1-\rho}} \tag{8}$$

Where $\omega$ is the utility weight attached to consumption, $\beta$ is the discount factor, $\sigma > 0$ is the risk aversion parameter, $\psi > 0$ is the elasticity of inter-temporal substitution (EIS) parameter with $\rho = \frac{1}{\psi}$ and $L_t = \left(L_{b,t}^{1+\rho_l} + L_{g,t}^{1+\rho_l}\right)^{\frac{1}{1+\rho_l}}$ is the labor composite, being $\rho l$ the elasticity of substitution.

The budget constraint for the Household is:

$$c_t + D_{t+1} = w_{b,t}L_{b,t} + w_{g,t}L_{g,t} + T_t + R_t D_t + \Pi_{t,g} + \Pi_{t,b} + \Phi_t \tag{9}$$

With $c_t$ is the consumption in period $t$, $L_{t,k}$ are the amount of hours supplied to each sector (green and brown), $w_{k,t}$ is the real wage paid to the Households. $\Phi_t$ are profits from the ownership of non-financial firms that will serve as start-up funds for the new bankers, $\Pi_{t,k}$ are the profit for non-financial firms, and $T_t$ are lump sum taxes. Also, I assume that intermediary deposits and government bonds are one-period bonds so that $R_t D_t$ are the interest received on deposits, and $D_{t+1}$ are the decision on the amount of deposit in each period.

We assume, as in Gertler and Karadi (2011), that a fraction $1 - f$ of household members are workers, while the remaining fraction $f$ are bankers. Over time, individuals can transition between these two occupations. Specifically, a banker in the current period remains a banker in the next period with probability $\chi$, independent of their past occupation history, including the duration for which they have been a banker.

The recursive representation of the Household problem is:

$$V_t = \max_{c_t, L_t, D_{t+1}} \left((1-\beta)\ \left(\left(c_t{}^{\omega}\ (1-L_t)^{1-\omega}\right)^{1-\rho} - \alpha_0 X_t^{1-\rho}\right) + \beta\left[(\mathbb{E}_t(V_{t+1}^{1-\sigma}))^{\frac{1}{1-\sigma}}\right]^{1-\rho}\right)^{\frac{1}{1-\rho}}$$

$$\text{s.t.} \quad c_t + D_{t+1} = w_{b,t}L_{b,t} + w_{g,t}L_{g,t} - T_t + R_t D_t + \Pi_{g,t} + \Pi_{b,t} + \Phi_t$$

$$L_t = \left(L_{b,t}^{1+\rho_l} + L_{g,t}^{1+\rho_l}\right)^{\frac{1}{1+\rho_l}}$$

The First order conditions of this problem give us the following equations:

Labor supply conditions:

$$(1-L_t)\left(L_{b,t}^{1+\rho_l}+L_{g,t}^{1+\rho_l}\right)^{\frac{\rho_l}{1+\rho_l}} L_{b,t}^{\rho_l}=\frac{c_t}{w_{b,t}}\frac{1-\omega}{\omega}$$

$$(1-L_t)\left(L_{b,t}^{1+\rho_l}+L_{g,t}^{1+\rho_l}\right)^{\frac{\rho_l}{1+\rho_l}} L_{g,t}^{\rho_l}=\frac{c_t}{w_{g,t}}\frac{1-\omega}{\omega}$$

The Stochastic Discount Factor is:

$$M_{t,t+1}=\beta\frac{C_t}{C_{t+1}}\frac{\left(C_{t+1}^{\omega}(1-L_{t+1})^{1-\omega}\right)^{1-\rho}}{\left(C_t^{\omega}(1-L_t)^{1-\omega}\right)^{1-\rho}}\left(\frac{V_{t+1}^{1-\sigma}}{\mathbb{E}_t\left(V_{t+1}\right)^{1-\sigma}}\right)^{\frac{\rho-\sigma}{1-\sigma}}$$

And the Euler Equation:

$$\mathbb{E}_t M_{t,t+1}R_{t+1}=1$$

### 5.2 Final Goods Producers

The representative final-good firm uses a standard CES aggregator to produce the final good $Y_t$:

$$Y_t=\left[\int_0^1 y_t(i)^{\frac{\epsilon-1}{\epsilon}}\right]^{\frac{\epsilon}{\epsilon-1}} \tag{10}$$

where the intermediate good produced by the intermediate firm $i$ is $y_t(i)$ sold at price $p_t(i)$. The final goods firm solves:

$$\max\ P_tY_t-\int_0^1 p_t(i)y_t(i)di$$

$$\text{s.t}\quad Y_t=\left[\int_0^1 y_t(i)^{\frac{\epsilon-1}{\epsilon}}\right]^{\frac{\epsilon}{\epsilon-1}}$$

With $P_t$ being the price level. The solution to this problem is the demand function for each firm $i$:

$$y_t(i)=y_t\left(\frac{p_t(i)}{p_t}\right)^{-\epsilon} \tag{11}$$

### 5.3 Intermediate Producers

We have a continuum of intermediate firms $i$, producing a differentiated input using a CES bundle of green $y_{g,t}$ and brown $y_{b,t}$ goods:

$$y_t(i) = \left[ (1-\zeta)^{\frac{1}{\gamma}} (y_{g,t}(i))^{\frac{\gamma-1}{\gamma}} + \zeta^{\frac{1}{\gamma}} (y_{b,t}(i))^{\frac{\gamma-1}{\gamma}} \right] \tag{12}$$

Where $\zeta$ is the share of brown goods in total output and $\gamma$ is the elasticity of substitution between brown and green goods:

The intermediate firm $i$ faces two optimization problems: an intertemporal problem for determining the optimal input combination and an intertemporal problem for setting the price. The primary objective is to minimize costs while ensuring a given level of production:

$$\min \; p_{g,t} y_{g,t}(i) + p_{b,t} y_{b,t}(i)$$

$$\text{st} \; \; y_t(i) = \left[ (1-\zeta)^{\frac{1}{\gamma}} (y_{g,t}(i))^{\frac{\gamma-1}{\gamma}} + \zeta^{\frac{1}{\gamma}} (y_{b,t}(i))^{\frac{\gamma-1}{\gamma}} \right]$$

Where $p_{g,t}$ represents the price of green production and $p_{b,t}$ denotes the price of brown production, both expressed relative to the price level $P_t$, the optimization problem results in the following demand functions for the green and brown inputs:

$$y_{g,t} = (1-\zeta) \left( \frac{p_{g,t}}{MC_t} \right)^{-\gamma} y_t(i) \tag{13}$$

$$y_{b,t} = \zeta \left( \frac{p_{b,t}}{MC_t} \right)^{-\gamma} y_t(i) \tag{14}$$

In this monopolistic competition setting, firms have the autonomy to set prices based on the demand they face from the final-good firm (4). When adjusting their price inflation concerning the Central Bank target inflation, firm $i$ incurs quadratic adjustment costs à la Rotemberg (1982). Therefore, the intertemporal problem for firm $i$ is:

$$\max_{\{p_t(i)\}_{i=0}^{\infty}} \; E_0 \left[ M_{t,0} \left( \left( \frac{p_t(i)}{P_t} \right)^{-\epsilon} \left( \frac{p_t(i)}{P_t} - MC_t \right) - \frac{\kappa_p}{2} \left( \frac{p_t(i)}{p_{t-1}(i)} - \bar{\pi} \right)^2 y_t \right) \right]$$

From a symmetric equilibrium, I get the standard Philips Curve:

$$\pi_t(\pi_t - \bar{\pi}) =_t \left[ M_{t,t+1}\pi_{t+1}(\pi_{t+1} - \bar{\pi})\frac{y_{t+1}}{y_t} \right] + \frac{\epsilon}{\kappa_P}\left( MC_t - \frac{\epsilon - 1}{\epsilon} \right) \tag{15}$$

Where the marginal cost is $MC_t = \left[ (1-\zeta)p_{g,t}^{1-\gamma} + \zeta p_{b,t}^{1-\gamma} \right]^{\frac{1}{1-\gamma}}$

### 5.4 Green and Brown producers

In this part of the model, I introduce environmental externalities as an aggregate damage cost affecting firm productivity. Following Heutel (2012), firms operate under a Cobb-Douglas production function, where pollution negatively impacts output through a damage function inspired by Nordhaus (2017):

$$y_{k,t} = A_t(\xi_{k,t}K_{t-1,k})^{\alpha} L_{t,k}^{1-\alpha} \tag{16}$$

Here, $A_t$ represents total factor productivity in sector $k$, and is affected by the stock of pollution $X_t$ as follows:

$$A_t = \left(1 - (D_0 + D_1 X_t + D_2 X_t^2)a\right) \tag{17}$$

This damage function, standard in DICE models (Nordhaus, 2008), captures the productivity loss from pollution. The variable $a$ denotes a TFP shock that follows an AR(1) process.

To model the accumulation of pollution, I assume that only the brown sector emits pollutants. The law of motion for the pollution stock is given by:

$$X_t = (1 - \delta_x)X_{t-1} + e_t + e^* \tag{18}$$

where $e_t$ is the domestic emission from brown firms, $\delta_x$ is the natural decay rate, and $e^*$ represents exogenous emissions from the rest of the world.

Emissions evolve with output, depending on the firm's abatement effort $ab_t$ and the elasticity of emissions $1 - \lambda$:

$$e_t = (1 - ab_t) y_{b,t}^{1-\lambda} \tag{19}$$

Brown firms maximize profits by choosing capital, labor, and abatement. They issue bonds $b_{b,t}$ to finance capital purchases: $b_{b,t} = q_{b,t} K_{b,t}$. Firms are also subject to a carbon tax on emissions and face a convex abatement cost:

$$Z_t = \left[ \theta_1 ab_t^{\theta_2} + \frac{1}{2} \kappa_e (ab_t - ab_{t-1})^2 \right] y_{b,t} \tag{20}$$

Here, $\theta_1$ and $\theta_2$ govern the cost-efficiency of abatement, and $\kappa_e$ captures adjustment costs. These dynamic costs prevent abrupt changes in emissions following policy shocks. Without them, models such as Carattini et al. (2023) predict an immediate transition to the new emissions steady state after implementing a carbon tax.[2]

Hence, the maximization problem for the brown firms is:

$$\max \;\; p_{b,t} y_{b,t} - w_{b,t} L_{b,t} - r_{kb,t} K_{b,t-1} - \tau_t e_t - Z_t$$

With $r_{k,b,t} = r_{b,t} q_{b,t-1} - (1-\delta) q_{b,t}$ being the rental rate of capital for brown firms and $\xi_{b,t}$ is a capital quality shock that follows an AR(1) process. The first-order conditions for this problem are:

$$(1-\alpha) y_{b,t} \left( p_{b,t} - \tau_t (1 - ab_t)(1-\lambda) y_{b,t}^{-\lambda} - \kappa_e (ab_t - ab_{t-1}) \right) = L_{b,t} w_{b,t}$$

$$\alpha y_{b,t} \left( p_{b,t} - \tau_t (1 - ab_t)(1-\lambda) y_{b,t}^{-\lambda} - \kappa_e (ab_t - ab_{t-1}) \right) = \xi_{b,t} k_{b,t-1} r_{k,b,t}$$

$$ab_t = \frac{\left( \tau_t y_{b,t}^{-\lambda} + \kappa_e ab_{t-1} + \kappa_e y_{b,t-1}/y_{b,t} ab_{t+1} \right)}{\theta_2 \theta_1 ab_t^{(\theta_2 - 2)} + \kappa_e (1 + y_{b,t+1}/y_{b,t})}$$

Analogously, green firms are not subject to the carbon tax or abatement costs, so the first-order conditions for these firms are:

$$(1-\alpha) y_{g,t} p_{g,t} = L_{g,t} w_{g,t}$$

[2]The inclusion of abatement adjustment costs ensures a smoother and more realistic emissions trajectory.

$$\alpha y_{g,t} p_{g,t} = \xi_{g,t} k_{g,t-1} r_{k,g,t}$$

### 5.5 Capital Producers

Capital producers acquire the output generated by final-good firms and non-depreciated capital from intermediate firms to facilitate physical capital production and face investment adjustment costs. Subsequently, green and brown firms purchase the capital. Capital producers solve:

$$\max_0 \sum_{i=0}^{\infty} M_{0,t} \sum_{k=b,g} \left[ q_{k,t} k_{k,t} - (1-\delta) q_{k,t} k_{k,t-1} - i_{k,t} \right]$$

$$\text{s.t. } k_{k,t} = (1-\delta) k_{k,t-1} + \left[ 1 - \frac{\kappa_I}{2} \left( \frac{i_{k,t}}{i_{k,t-1}} - 1 \right)^2 \right] i_{k,t}$$

Where $i_{k,t}$ is the investment in each sector $k = g, b$. The first-order conditions for each type of capital are:

$$1 = q_{k,t} \left( 1 - \frac{\kappa_I}{2} \left( \frac{i_{k,t}}{i_{k,t-1}} - 1 \right)^2 - \frac{i_{k,t}\, \kappa_I \left( \frac{i_{k,t}}{i_{k,t-1}} - 1 \right)}{i_{k,t-1}} \right) + {}_t M_{t,t+1}\, \kappa_I\, q_{k,t+1} \left( \frac{i_{k,t+1}}{i_{k,t}} - 1 \right) \left( \frac{i_{k,t+1}}{i_{k,t}} \right)^2$$

### 5.6 Financial Intermediaries

We incorporate financial frictions via a borrowing constraint on banks, following Ferrari and Nispi Landi (2024) and Carattini et al. (2023). These frictions, modeled through an agency problem, allow the framework to capture key macroeconomic dynamics of transition risk. As shown in Carattini et al. (2023), economies with financial frictions experience deeper recessions during green transitions compared to frictionless models.

Credit frictions matter because policy shocks—like a carbon tax—reduce the value of brown-sector assets, weakening bank balance sheets and tightening credit. This amplifies the real effects of climate policies via higher risk premia and lower investment.

Banks raise household deposits and lend to green and brown firms. Their balance sheet is:

$$b^f_{g,t} + b^f_{b,t} = NW_t + D_t \tag{21}$$

where $b^f_{k,t}$ are bond holdings, $NW_t$ is bank net worth, and $D_t$ are deposits. To capture frictions in portfolio reallocation, banks face a quadratic cost when deviating from the steady-state share of green bonds $b^*$.

This cost introduces a wedge between green and brown returns, slowing banks' portfolio adjustment in response to policy or market shifts. Net worth evolves as:

$$NW_t = r_{g,t} b^f_{g,t-1} + r_{b,t} b^f_{b,t-1} - \frac{r_{t-1}}{\pi_t} D_{t-1} - \frac{\kappa_F}{2} NW_{t-1} \left( \frac{b^f_{g,t-1}}{b^f_{t-1}} - b^* \right)^2 \tag{22}$$

or equivalently:

$$\frac{NW_t}{NW_{t-1}} = \left( r_{g,t} - \frac{r_t}{\pi_{t+1}} \right) b^f_{g,t-1} + \left( r_{b,t} - \frac{r_t}{\pi_{t+1}} \right) b^f_{b,t-1} - \frac{r_t}{\pi_{t+1}} - \frac{\kappa_F}{2} \left( \frac{b^f_{g,t-1}}{b^f_{t-1}} - b^* \right)^2 \tag{23}$$

To prevent over-leveraging, I assume an agency friction à la Gertler and Karadi (2011), where depositors enforce:

$$V^f_t \geq \theta_t (b^f_{g,t} + b^f_{b,t}) \tag{24}$$

with $\theta_t$ being the fraction of assets the banker can divert. With probability $1 - \chi$, bankers exit and transfer net worth to households. With probability $\chi$, they remain, and their value is:

$$V^f_t = \max_t \left[ \sum_{i=0}^{\infty} (1 - \chi) \chi^i M_{t,t+i} NW_{t+1+i} \right] \tag{25}$$

We assume this constraint binds. The bank maximizes $(16)$ subject to $(14)$ and $(15)$, leading to first-order conditions:

$$lev_t = \frac{M_{t,t+1} \nu_{t+1} \left( \frac{r_t}{\pi_{t+1}} + (r_{g,t+1} - r_{b,t+1}) lev_{g,t} - \frac{\kappa_F}{2} \left( \frac{lev_{g,t}}{lev_t} - b^* \right)^2 \right)}{\theta - M_{t,t+1} \nu_{t+1} \left( r_{b,t+1} - \frac{r_t}{\pi_{t+1}} \right)}$$

$$_t M_{t,t+1} \nu_{t+1} \left[ r_{g,t+1} - r_{b,t+1} - \left( \frac{lev_{g,t}}{lev_t} - b^* \right) \frac{\kappa_F}{lev_t} \right] = 0$$

where $lev_t = \frac{b^f_t}{NW_t}$ is leverage, $lev^g_t = \frac{b^f_{g,t}}{NW_t}$ is green leverage, and $\nu_t$ is the bank's continuation

value:

$$\nu_t = 1 - \chi + \chi_t M_{t,t+1} \left[ \frac{r_t}{\pi_{t+1}} + (r_{g,t+1} - r_{b,t+1}) lev_{g,t} + lev_t \left( r_{b,t+1} - \frac{r_t}{\pi_{t+1}} \right) - \frac{\kappa_F}{2} \left( \frac{lev_{g,t}}{lev_t} - b^* \right)^2 \right]$$

Aggregate net worth consists of continuing and new bankers: $NW_t = NW_{e,t} + NW_{n,t}$. Continuing bankers evolve as:

$$NW_{e,t} = \chi \left[ (r_{g,t} - r_{b,t}) lev^g_{t-1} + (r_{b,t} - \frac{r_{t-1}}{\pi_t}) lev_{t-1} + \frac{r_{t-1}}{\pi_t} - \frac{\kappa_F}{2} \left( \frac{lev^g_{t-1}}{lev_{t-1}} - b^* \right)^2 \right] NW_{t-1} \quad (26)$$

New bankers receive $\iota b^f_t$ as start-up funding: $NW_{n,t} = \iota b^f_t$. Hence, aggregate net worth evolves as:

$$NW_t = \chi \left( \frac{r_{t-1}}{\pi_t} + (r_{b,t} - \frac{r_{t-1}}{\pi_t}) lev_{t-1} + (r_{g,t} - r_{b,t}) lev^g_{t-1} - \frac{\kappa_F}{2} \left( \frac{lev_{g,t-1}}{lev_{t-1}} - b^* \right)^2 \right) NW_{t-1} + \iota b^f_t$$

### 5.7 Central Banks and Government

### 5.8 Monetary Policy and Final Goods Market Clearing

Monetary policy is conducted through a standard Taylor rule with interest rate smoothing, capturing how the central bank adjusts the nominal interest rate in response to deviations of inflation and output from their respective targets:

$$\frac{r_t}{\overline{r}} = \left( \frac{r_{t-1}}{\overline{r}} \right)^{\rho_r} \left[ \left( \frac{\pi_t}{\overline{\pi}} \right)^{\rho_\pi} \left( \frac{Y_t}{\overline{Y^*}} \right)^{\rho_y} \right]^{1-\rho_r} e_t^{m_t} \quad (27)$$

Here, $r_t$ is the nominal risk-free interest rate, and $\overline{r}$ is its steady-state level. Inflation is denoted by $\pi_t$, with $\overline{\pi}$ as the central bank's target. $Y_t$ represents real output, while $\overline{Y^*}$ is the potential output . The parameter $\rho_r \in (0, 1)$ controls the degree of interest rate smoothing, ensuring gradual adjustments over time. The policy parameters $\rho_\pi$ and $\rho_y$ capture the responsiveness to inflation and output gaps, respectively. The term $e_t^{m_t}$ introduces monetary policy shocks that follows an

AR(1) process, allowing for unexpected deviations in the interest rate path.

To close the model, I impose the final goods market clearing condition, which equates total output to the sum of its uses:

$$y_t = c_t + I_t + \frac{\kappa_F}{2} NW_{t-1} \left( \frac{b^f_{g,t-1}}{b^f_{t-1}} - b^* \right)^2 + \frac{\kappa_p}{2} \left( \frac{p_t(i)}{p_{t-1}(i)} - \bar{\pi} \right)^2 y_t \tag{28}$$

### 5.9 Uncertainty Shocks

To capture the role of transition-related uncertainty, I introduce two types of stochastic shocks that affect key components of the model. These shocks influence firm decisions, household expectations, and ultimately the macroeconomic response to climate policies.

First, I introduce a Capital Quality Shock to the brown sector to capture uncertainty about the future valuation of carbon-intensive capital in response to the Climate Policy Uncertainty. This shock reflects the risk that future climate regulations may suddenly reduce the productivity or value of brown-sector assets.

Formally, I model the capital quality of the brown sector, $\xi_{b,t}$, as a stochastic process subject to time-varying volatility:

$$\log(\xi_{b,t}) = \rho_\xi \log(\xi_{b,t-1}) + \sigma_{\xi,t} \varepsilon_{\xi,t} \tag{29}$$

where $\sigma_{\xi,t}$ evolves according to:

$$\log(\sigma_{\xi,t}) = (1 - \rho_\sigma) \log(\bar{\sigma}_\xi) + \rho_\sigma \log(\sigma_{\xi,t-1}) + \sigma_{\sigma\xi,t} \eta_{\xi,t} \tag{30}$$

This specification follows the uncertainty shock structure in Basu and Bundick (2017), where second-moment shocks (to volatility) affect precautionary behavior. A rise in $\sigma_{\xi,t}$ implies greater uncertainty over capital effectiveness, leading to precautionary reductions in investment and borrowing by brown firms.

Then, I allow for stochastic variation in the carbon tax rate $\tau_t$, reflecting policy uncertainty over the timing and stringency of climate regulation:

$$\log(\tau_t) = \rho_\tau \log(\tau_{t-1}) + \sigma_{\tau,t} \varepsilon_{\tau,t} \tag{31}$$

$$\log(\sigma_{\tau,t}) = (1-\rho_\sigma)\log(\bar{\sigma}_\tau) + \rho_\sigma \log(\sigma_{\tau,t-1}) + \sigma_{\sigma\tau,t}\eta_{\tau,t} \tag{32}$$

Uncertainty about future carbon taxes raises the perceived cost of brown-sector investment and may alter bank portfolio choices through expected future returns and risk premia.

These uncertainty shocks are central to the analysis of climate transition risks. Under Epstein-Zin preferences, agents respond not only to first-moment shocks but also to volatility, amplifying the impact of uncertainty on precautionary savings, investment, and portfolio allocation.

The uncertainty parameters are disciplined by matching the impulse-response functions (IRFs) produced by the DSGE model to the empirical IRFs obtained from local projections. Denote by $\widehat{\psi}_{hv}$ the empirical response of variable $v = 1, \ldots, V$ at horizon $h = 0, \ldots, H$ and by $\psi_{hv}(\theta)$ the corresponding model response, which is a nonlinear function of the parameter vector $\theta$. Estimation minimizes the quadratic distance

$$\widehat{\theta} = \arg\min_{\theta} \; J(\theta), \qquad J(\theta) \;=\; \big[\mathrm{vec}\big(\psi(\theta) - \widehat{\psi}\big)\big]' W \; \mathrm{vec}\big(\psi(\theta) - \widehat{\psi}\big),$$

where $\mathrm{vec}(\cdot)$ stacks the $(H+1)\times V$ IRF matrix column-wise and $W$ is a positive-definite weighting matrix. The baseline choice sets $W$ to a diagonal matrix with elements equal to the inverse empirical variance of each $\widehat{\psi}_{hv}$, weighting more precise responses more heavily while remaining agnostic about cross-covariances.

For a given $\theta$ the routine solves the model at third order with pruning, simulates the stochastic steady state, and extracts the resulting IRFs. The distance function is minimized with a derivative-free Nelder–Mead algorithm initialized at multiple starting points, a strategy shown to work well in macro-finance calibration exercises (Christiano et al., 2014). The estimated parameters therefore reproduce not only first moments but also the dynamic response of key real and financial variables to a climate-policy-uncertainty innovation, anchoring the volatility and persistence of the uncertainty shocks directly in the data rather than selecting them ad hoc.

### 5.10 Calibration

The model is calibrated to match key features of the US economy at a quarterly frequency. The parameterization draws upon established values from the literature, particularly Ferrari and Nispi Landi (2024), Barrage (2020), Carattini et al. (2023), and Gertler and Karadi (2011). Table 1 summarizes

the baseline parameter values, with comprehensive details on the calibration strategy, especially for targeted parameters, provided in Appendix B.

**Table 1:** Macroeconomic and Household Parameters

| Parameter | Description | Value | Source |
|---|---|---|---|
| $\beta$ | Discount factor | 0.995 | Standard |
| $\alpha$ | Capital share in production | 0.36 | Coenen et al. (2018) |
| $\psi$ | Intertemporal elasticity of substitution | 0.5 | Standard |
| $\sigma$ | Risk aversion coefficient | 2 | Carattini et al. (2023) |
| $\omega$ | Weight of consumption in utility | 0.32 | Barrage (2020) |
| $\delta$ | Capital depreciation rate | 2.5% | Standard |
| $\rho_l$ | Elasticity of substitution for labor hours | 1 | Carattini et al. (2023) |
| $\gamma$ | Elasticity of substitution for brown and green goods | 2 | Carattini et al. (2023) |
| $\zeta$ | Weight of brown goods in consumption | 0.8 | Giovanardi et al. (2023) |
| $\kappa_p$ | Price adjustment cost | 70 | Match Calvo = 0.82 |
| $\bar{\pi}$ | Target inflation rate | 1.005 | Coenen et al. (2018) |
| $\kappa_I$ | Investment adjustment cost | 10.78 | Coenen et al. (2018) |
| $\bar{r}$ | Steady-state nominal interest rate | 1.01 | Coenen et al. (2018) |
| $\rho_r$ | Interest rate smoothing parameter in Taylor rule | 0.93 | Coenen et al. (2018) |
| $\rho_\pi$ | Inflation responsiveness in Taylor rule | 2.74 | Coenen et al. (2018) |
| $\rho_y$ | Output gap responsiveness in Taylor rule | 0.03 | Coenen et al. (2018) |
| $\rho_a$ | Persistence of technology shock | 0.93 | Coenen et al. (2018) |
| $\rho_\xi$ | Persistence of capital quality shock | 0.66 | Gertler and Karadi (2011) |

Several standard macroeconomic parameters are adopted from the NAWM-II model, originally calibrated for the Euro Area. We assume these values are sufficiently similar for the US context. These include the capital share in production, the elasticity of substitution between differentiated goods, the target inflation rate, investment adjustment costs, the bank survival probability, and parameters governing the Taylor rule and the productivity process. Following Ferrari and Nispi Landi (2024), the discount factor $\beta$ is set to achieve a steady-state annualized real interest rate of 2% on public debt. Additionally, $\theta$ is calibrated to yield a steady-state total bank leverage ratio of 6, and $\iota$ is chosen to match an annualized steady-state corporate spread of 2.17%. The price stickiness parameter $\kappa_p$ corresponds to a Calvo probability of 0.82, consistent with NAWM-II.

Household preference parameters are informed by Barrage (2020) for the consumption utility weight. The pollution disutility parameter is calibrated internally to align with the specified production damage function, as detailed in Appendix B.

For the environmental block parameters, we follow the methodology outlined in Gibson and Heutel (2023) and implemented by Ferrari and Nispi Landi (2024).

**Table 2:** Environmental and Financial Sector Parameters

| Parameter | Description | Value | Source |
|---|---|---|---|
| $D_0$ | Constant term in damage function | -0.0076 | Gibson and Heutel (2023) |
| $D_1$ | Linear term in damage function | $9.0182 \times 10^{-7}$ | Gibson and Heutel (2023) |
| $D_2$ | Quadratic term in damage function | $1.2013 \times 10^{-10}$ | Gibson and Heutel (2023) |
| $\delta_x$ | Pollution decay rate | 0.0035 | Gibson and Heutel (2023) |
| $e^{\text{row}}$ | Constant emissions level | 25.11 | Gibson and Heutel (2023) |
| $\lambda$ | Convexity parameter of the emission function | 0.4 | Gibson and Heutel (2023) |
| $\kappa_F$ | Bank portfolio adjustment cost | $10^{-4}$ | Ferrari and Nispi Landi (2024) |
| $b^*$ | Steady-state share of banks' green bonds | 0.2 | Market Neutrality |
| $\theta$ | Divertible portion of assets | 0.4474 | Match $lev_{ss} = 6$ |
| $\chi$ | Banks' survival probability | 0.972 | Gertler and Karadi (2011) |
| $\iota$ | Wealth share for new banks | 0.002 | Gertler and Karadi (2011) |
| $\mu_{ss}$ | Steady-state central bank bond holdings | 1.35% | Ferrari and Nispi Landi (2024) |
| $\mu_{gss}$ | CB share of green bonds | 0.2 | Market Neutrality |

Finally, concerning the substitutability between energy inputs, we adopt $\gamma = 2$ from Carattini et al. (2023), indicating imperfect substitution between green and brown goods. Consistent with Giovanardi et al. (2023), the weight assigned to the brown good in the composite is $\zeta = 0.8$.

### 5.11 Solution Method

The objective of this analysis is to examine the effects of an increase in the second moment of two critical shock processes: the Brown Capital Quality shock and the Carbon Tax shock. Following the methodology outlined by Fernández-Villaverde et al. (2015), accurately capturing the impulse responses to such second-moment shocks requires employing at least a third-order approximation of the model's policy functions. For this, I use Dynare, which computes rational expectations solutions via a third-order Taylor series approximation around the deterministic steady state.

The impulse response functions (IRFs) are generated through a simulation procedure. Initially, the model is simulated under a baseline scenario without shocks, resulting in a trajectory from which I extract the stochastic steady state—an equilibrium reference accounting for inherent model uncertainty. This baseline is essential as it serves as a benchmark, allowing subsequent responses to be clearly interpreted as deviations caused exclusively by the introduced shocks.

Subsequently, a timed one-unit shock to either the uncertainty surrounding brown capital quality or the carbon tax is introduced immediately following the burn-in phase. This precise timing facilitates a clear observation of the dynamic adjustments and propagation mechanisms within the model.

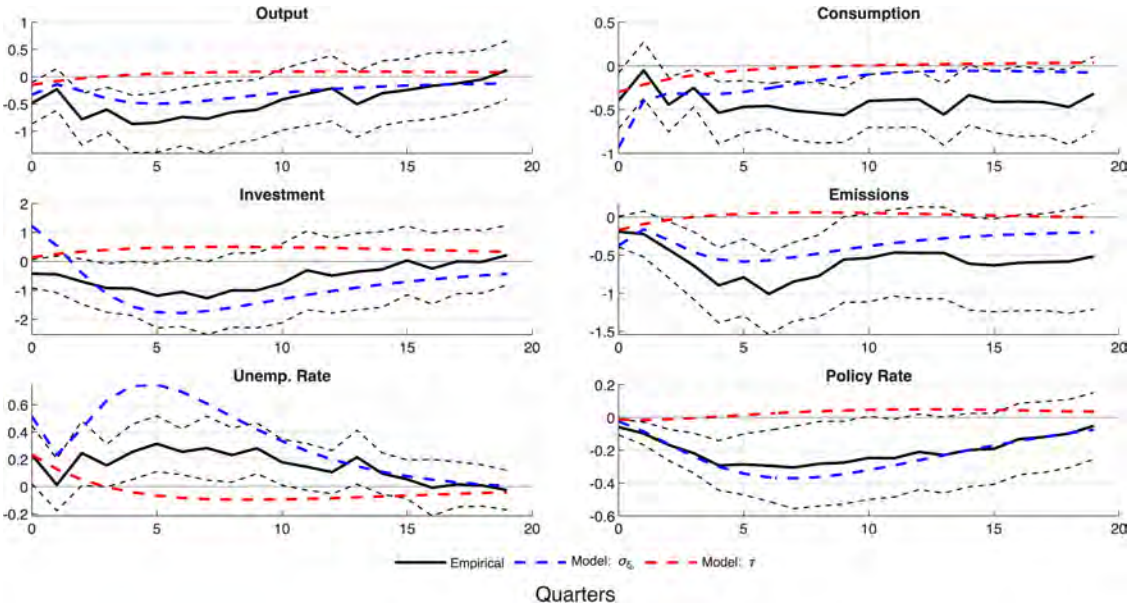
By implementing this procedure, I can isolate the specific transmission channels through which uncertainty shocks influence the economy, providing insights into their short-term and medium-term implications.

# 6 Quantitative Results

This section presents the Impulse Response Functions (IRFs) generated by the model, highlighting key variables identified in the empirical analysis. These IRFs show the reactions to two types of shocks: uncertainty about the quality of brown capital and an increase in the carbon tax. The model parameters were chosen using the IRF matching method.

Figure 6 contrasts the empirical LP IRFs (black) with the model's responses to two pure volatility (second-moment) shocks: a brown-capital quality volatility shock (blue, "asset-quality") and a carbon-tax volatility shock red, "tax-vol").

**Figure 6:** Empirical and Theoretical IRF - Key Outcome Variables




Units are percent deviations from the stochastic steady state; horizontal axis in quarters.

The empirical IRFs after a CPU shock display a recession-like pattern: output, consumption, and investment fall; unemployment rises; the policy rate eases; and emissions decline. When I confront the model with these facts, the *brown–capital quality volatility* shock, $\sigma_{\sigma_\xi}$ (blue), tracks the data closely. It generates an immediate and persistent drop in activity, a hump-shaped increase in unemployment, and a sustained policy-rate easing (the same co-movement seen in the LPs). By contrast, a *carbon–tax volatility* shock, $\sigma_{\sigma_\tau}$ (red), moves the economy in the opposite direction on most margins: aggregate activity nudges up, investment rises, unemployment drifts down, and the policy rate edges higher. In short, $\sigma_\tau$ behaves like a reallocation disturbance with little aggregate drag, while $\sigma_\xi$ replicates a broad contraction.

Magnitudes and timing reinforce this message. Under $\sigma_\xi$, investment bottoms out around 6–8 quarters and recovers only slowly. Output and consumption follow a similarly persistent path, emissions fall modestly but durably. These dynamics mirror the empirical responses. Under $\sigma_{\sigma_\tau}$, movements are small and short-lived, failing to match either the depth or the duration of the downturn in the data.

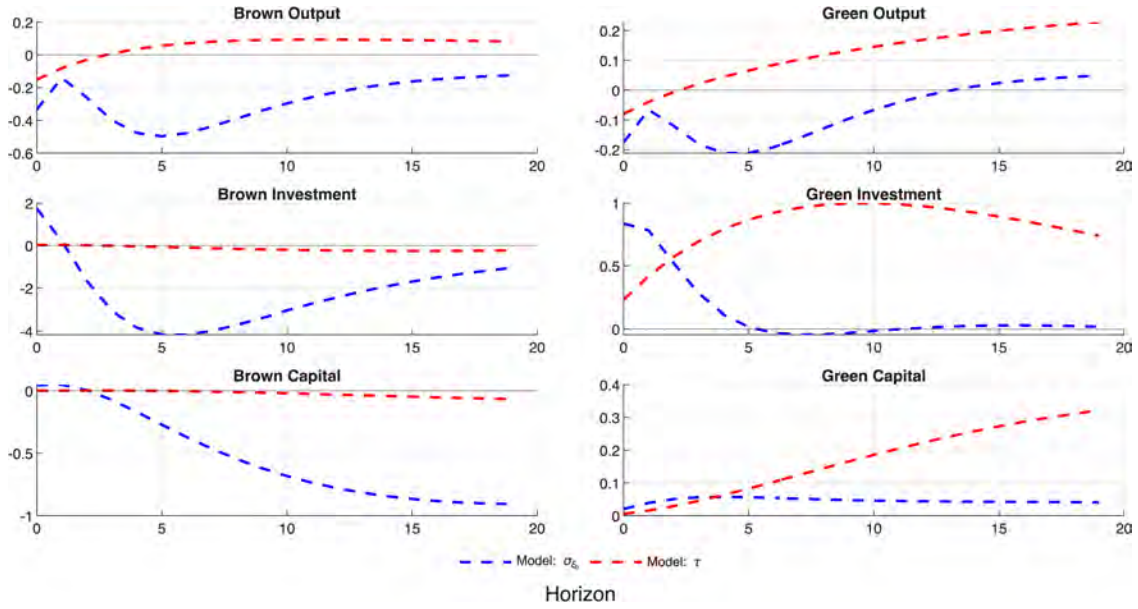
The sectoral decomposition clarifies why. With $\sigma_{\sigma_\xi}$, *brown* output and investment drop sharply and the brown capital stock erodes, while *green* activity initially softens and only recovers gradually. That pattern is consistent with the LP evidence: total investment contracts, fossil-fuel produc-

tion falls, and renewables improve but not explosively (credit headwinds spill over to both sectors). With $\sigma_{\sigma_\tau}$, instead, green investment and capital surge while brown barely declines (and can even tick up). This looks like apolicy-salience/stringency narrative, strong expected incentives for clean technologies rather than an uncertainty shock. It aligns with findings that environmental-policy news can lift clean investment and pressure brown returns (Noailly et al., 2024, 2022), but it conflicts with the central empirical regularity here: CPU spikes are accompanied by a macro contraction (Palikhe et al., 2024; Noailly et al., 2022)

Interpreted through the broader uncertainty literature, $\sigma_{\sigma_\xi}$ is the natural candidate. Uncertainty that targets the pledgeability and resale value of brown assets, tightens borrowing constraints, compresses Tobin's $q$ for carbon-intensive capital ($q^B$), and propagates through credit markets, being this precisely the amplification emphasized by financial-frictions literature (Gilchrist et al., 2014). With nominal rigidities, tighter financial conditions translate into demand-side comovement Basu and Bundick, 2017; Bloom et al., 2018. The resulting decline in fossil activity delivers the observed drop in emissions, consistent with evidence that climate-policy risk is associated with lower $CO_2$ (Gavriilidis, 2021). The tax–volatility shock, by contrast, primarily reallocates toward green without producing the broad tightening in credit and aggregate demand that the data reveal, a mismatch with evidence that environmental policy uncertainty restrains investment and external finance in exposed industries and young clean-tech firms.

(Noailly et al., 2022).

**Figure 7:** Empirical and Theoretical IRF - Sectoral Variables




Units are log-percent deviations from the stochastic steady state; horizontal axis in quarters.

In this case, a CPU shock behaves like a *second-moment, asset–quality hit to brown collateral*, not like volatility in tax rates per se. A small role for $\sigma_{\sigma_\tau}$ may help explain the modest, lagged lift in renewables, but the *center of gravity is the collateral channel*, the only mechanism that simultaneously delivers the contraction, the monetary easing, and the directional change in emissions seen in the empirical IRFs.

The core result is that uncertainty about the quality of brown capital propagates far more persistently through the financial system than uncertainty about future carbon-tax paths. When agents revise down the pledgeable value of existing brown assets, two mechanisms activate simultaneously. Collateral values fall, so banks raise haircuts and compress lending. At the same time, firms holding depreciated or harder-to-pledge capital postpone or cancel projects because they cannot finance new investment or refinance old positions at reasonable terms. This financial-accelerator channel produces the pattern we document in the data and in the baseline model: a protracted decline in output, investment, and loans, a sustained drop in emissions driven by weaker fossil activity, and an accommodative policy response of roughly one-half percentage point as monetary authorities counter the slump. The state-dependent evidence fits this view: the contraction is strongest when credit is expanding and collateral is actively used.

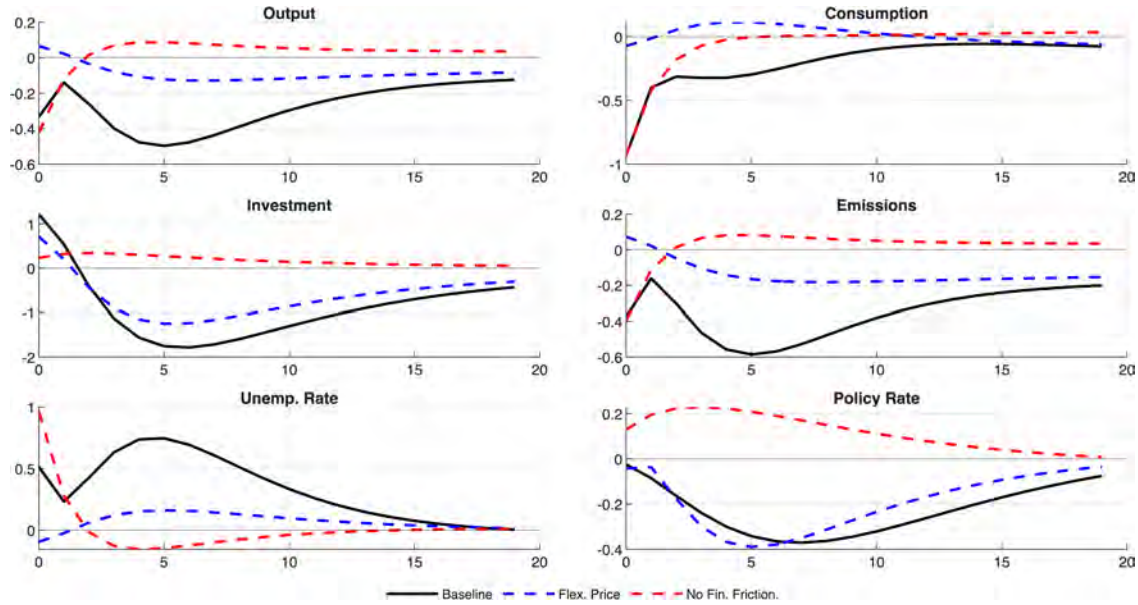
### 6.1 Role of nominal and financial frictions under capital-quality volatility

The baseline model with financial frictions and Rotemberg price adjustment costs produces a recession-like response after a rise in the volatility of brown-capital quality. On the real side, output, consumption, and total investment fall with a trough around six to eight quarters and a slow recovery. Unemployment rises with a hump and the policy rate eases persistently, consistent with a demand-driven contraction. Emissions decline as fossil activity retrenches. The sectoral IRFs show a sharp fall in brown investment and a steady erosion of the brown capital stock. Green activity dips on impact and then recovers only gradually. This pattern matches the empirical LPs and is consistent with the idea that higher uncertainty about pledgeable brown collateral compresses Tobin's q for brown assets, tightens borrowing constraints, and transmits through credit markets, a mechanism emphasized in financial-frictions as Gilchrist et al. (2014). With nominal rigidities in place, tighter financial conditions translate into comovement in output, consumption, and hours as in Basu and Bundick (2017).

Removing financial frictions fundamentally changes the propagation. Aggregate variables no longer display a meaningful contraction. Output and consumption quickly return to baseline or even tick up, unemployment barely moves, and the policy rate drifts upward rather than easing. At the sector level, green investment and capital rise while brown activity shows only a mild and short-lived decline. The shock operates mainly as a relative-price or portfolio reallocation disturbance without a credit amplifier. In the absence of collateral constraints, the capital-quality volatility does not depress aggregate demand, which explains the lack of monetary easing and the weak response of emissions. This experiment demonstrates that the collateral channel is necessary to generate the depth, persistence, and co-movement observed in the data and in the baseline model.

Allowing prices to be flexible while keeping financial frictions attenuates but does not eliminate the contraction. Output, consumption, and investment still fall on impact, yet the magnitudes are smaller, the unemployment response is muted, and the policy rate cuts are shallower and shorter. Brown investment declines less and green activity stabilizes more quickly. With flexible prices, relative prices adjust rapidly and part of the demand shortfall is absorbed through price movements rather than quantities. The financial wedge still tightens because brown collateral be-

**Figure 8:** Empirical and Theoretical IRF - Comparison of Models - Capital Quality Shock - Key Outcomes

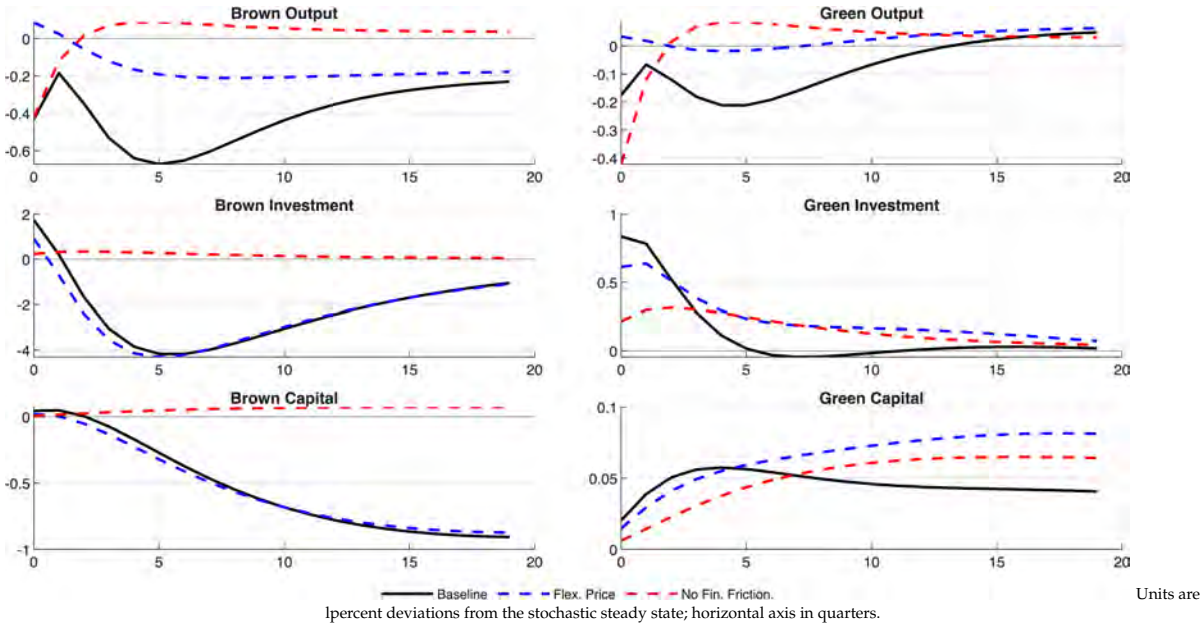



Units are percent deviations from the stochastic steady state; horizontal axis in quarters.

comes riskier, but the absence of nominal rigidities reduces the real amplification and weakens the comovement that characterizes the baseline. This mirrors the broader uncertainty literature where price stickiness is key for strong aggregate co-movement (Basu and Bundick, 2017).

Taken together, the three experiments deliver a clean message. The aggregate contraction and the slow recovery are driven by the interaction of a collateral shock with both credit frictions and nominal rigidities. Financial frictions are the first-order amplifier: without them the volatility shock mostly reallocates resources toward green production and cannot reproduce the decline in output, investment, and emissions or the monetary easing seen empirically. Price adjustment costs are the co-amplifier that convert tighter credit into broad demand weakness, stronger co-movement, and a persistent rise in unemployment. The baseline configuration therefore provides the closest qualitative match to the empirical impulse responses and to the findings in the literature that uncertainty shocks depress activity through credit and demand channels while inducing a modest decline in emissions through reduced fossil output.

**Figure 9:** Comparison of Models - Capital Quality Shock - Sector Outcomes




Units are lpercent deviations from the stochastic steady state; horizontal axis in quarters.

# 7 Implications for Policy and the Green Transition

Local projections and DSGE modeling show that climate policy uncertainty (CPU) drives macroeconomic effects through financial channels. When uncertainty reduces the pledgeable value of carbon-intensive (brown) capital, banks increase haircuts, credit tightens, investment falls, and a demand slowdown follows. Unlike carbon-tax volatility, which mainly shifts activity to cleaner technologies, CPU triggers recession-like effects. Policy should thus reduce volatility that erodes collateral while ensuring predictable decarbonization incentives.

The macroeconomic cost of the low-carbon transition is lowest when firms and lenders can anticipate policy paths. Clear carbon pricing schedules, transparent phase-out timelines for high-carbon assets, and stable support for clean investments reduce uncertainty. These measures prevent sudden collateral markdowns, limit credit contraction, and minimize output losses for a given emissions reduction.

CPU shocks act like negative demand disturbances, lowering output, investment, and inflation. Central banks should monitor CPU alongside credit spreads, incorporate transition risks into forecasts, and signal that monetary policy will counter demand slowdowns while prudential tools address financial stability. Preannounced collateral frameworks can avoid abrupt adjustments during CPU spikes.

In expansions, when credit and collateral use are high, supervisors should scrutinize banks with brown asset exposures, apply forward-looking haircuts, and stress-test asset value volatility. Targeted exposure limits and capital buffers curb risks without broad credit rationing. Standardized emissions disclosures enhance collateral valuation accuracy.

Fiscal policies should address financing frictions with stable, outcome-based incentives, such as credits for decarbonization or guarantees for brown-to-green retrofits. Public investment in infrastructure and streamlined permitting lower project risks. Place-based assistance and retraining programs mitigate regional and labor market disruptions, reducing political pressures that fuel uncertainty.

Coordinated action is critical. Climate authorities must ensure policy predictability, financial regulators should integrate transition risks into oversight, central banks should treat CPU as a demand shock while managing leverage, and fiscal policy should support low-carbon projects without subsidizing stranded assets. This alignment reduces emissions efficiently while sustaining access to finance.

# 8 Conclusions

This paper identifies and quantifies the macroeconomic effects of a distinct form of economic risk: Climate Policy Uncertainty (CPU). Through a series of empirical tests and a quantitative model, I show that CPU is not merely another name for aggregate financial or political uncertainty, but a unique shock with a specific transmission channel and a state-dependent impact on the U.S. economy.

The empirical analysis, using local projections on monthly U.S. data, proceeds in two steps. First, I show that, unconditionally, a CPU shock is a potent contractionary force, reducing investment and output. Unlike a generic financial uncertainty shock (proxied by the VIX or US-EPU), however, a CPU shock leads to a direct and significant decline in emissions. We trace this effect to its source: a sharp, targeted contraction in the industrial production of fossil fuels, while renewable energy production remains unharmed. This provides evidence that CPU operates through a sectoral reallocation channel.

The paper's core contribution comes from the second step: a state-dependent analysis that

reveals a stark asymmetry in this channel's potency. During economic expansions, when the unemployment rate is low, the CPU shock is disruptive, causing a significant fall in investment, production, and lending. During recessions, however, the same shock has no statistically significant effect on any major real or financial variable. This asymmetric impact and significant in expansions but weak in recessions—is a unique signature that differentiates CPU from standard uncertainty shocks, which remain contractionary in both states of the business cycle.

To rationalize these empirical facts, I develop a two-sector (green/brown) New Keynesian DSGE model with financial frictions and Epstein-Zin preferences. The model successfully reproduces general results observed in the data. It identifies the key mechanism: the sectoral reallocation channel from the Brown sector to the low-carbon sector. Also, the model suggests that uncertainty over the fundamental quality of carbon-intensive capital provides a better match for the data than uncertainty over the path of a carbon tax, indicating the role of the financial markets in shaping the transition to a low carbon economy.

These findings yield clear policy implications. First, macroeconomic stability is an essential enabler of the green transition; the market-driven reallocation from brown to green capital only occurs in healthy, expansionary economies. Second, the timing of major climate initiatives matters, presenting a trade-off between minimizing economic disruption (by legislating in a recession) and maximizing reallocative impact (by legislating in an expansion). Finally, policy design should aim to reduce ambiguity over the long-term relative returns of green versus brown capital, for instance through credible, long-term carbon pricing paths.

This research could be extended by using granular, firm-level data to test the sectoral reallocation mechanism more directly and by exploring the international spillovers of climate policy uncertainty from one economic bloc to another. Still, the evidence presented here establishes CPU as a distinct and important source of macroeconomic risk whose state-dependent nature has critical consequences for economic stability and the transition to a low-carbon economy.

## References


Ackerman, F., Stanton, E. A., and Bueno, R. (2013). Epstein–zin utility in dice: Is risk aversion irrelevant to climate policy? *Environmental and Resource Economics*, 56:73–84.

Auerbach, A. J. and Gorodnichenko, Y. (2012). Fiscal multipliers in recession and expansion. In *Fiscal policy after the financial crisis*, pages 63–98. University of Chicago Press.

Baker, S. R., Bloom, N., and Davis, S. J. (2016). Measuring economic policy uncertainty. *The quarterly journal of economics*, 131(4):1593–1636.

Baker, S. R., Bloom, N., Davis, S. J., and Kost, K. J. (2019). Policy news and stock market volatility. Technical report, National Bureau of Economic Research.

Barnichon, R. and Brownlees, C. (2019). Impulse response estimation by smooth local projections. *Review of Economics and Statistics*, 101(3):522–530.

Barrage, L. (2020). Optimal dynamic carbon taxes in a climate–economy model with distortionary fiscal policy. *The Review of Economic Studies*, 87(1):1–39.

Basu, S. and Bundick, B. (2017). Uncertainty shocks in a model of effective demand. *Econometrica*, 85(3):937–958.

Berestycki, C., Carattini, S., Dechezleprêtre, A., and Kruse, T. (2022). Measuring and assessing the effects of climate policy uncertainty.

Bernanke, B. S. (1983). Irreversibility, uncertainty, and cyclical investment. *The quarterly journal of economics*, 98(1):85–106.

Bloom, N. (2009). The impact of uncertainty shocks. *Econometrica*, 77(3):623–685.

Bloom, N., Floetotto, M., Jaimovich, N., Saporta-Eksten, I., and Terry, S. J. (2018). Really uncertain business cycles. *Econometrica*, 86(3):1031–1065.

Caldara, D. and Iacoviello, M. (2022). Measuring geopolitical risk. *American economic review*, 112(4):1194–1225.

Caldara, D., Iacoviello, M., Molligo, P., Prestipino, A., and Raffo, A. (2020). The economic effects of trade policy uncertainty. *Journal of Monetary Economics*, 109:38–59.

Carattini, S., Heutel, G., and Melkadze, G. (2023). Climate policy, financial frictions, and transition risk. *Review of Economic Dynamics*, 51:778–794.

Christiano, L. J., Motto, R., and Rostagno, M. (2014). Risk shocks. *American Economic Review*, 104(1):27–65.

Coenen, G., Karadi, P., Schmidt, S., and Warne, A. (2018). The new area-wide model ii: an extended version of the ecb's micro-founded model for forecasting and policy analysis with a financial sector.

Diluiso, F., Annicchiarico, B., Kalkuhl, M., and Minx, J. C. (2021). Climate actions and macro-financial stability: The role of central banks. *Journal of Environmental Economics and Management*, 110:102548.

Epstein, L. G. and Zin, S. E. (1991). Substitution, risk aversion, and the temporal behavior of consumption and asset returns: An empirical analysis. *Journal of political Economy*, 99(2):263–286.

Epstein, L. G. and Zin, S. E. (2013). Substitution, risk aversion and the temporal behavior of consumption and asset returns: A theoretical framework. In *Handbook of the fundamentals of financial decision making: Part i*, pages 207–239. World Scientific.

Fernández-Villaverde, J., Guerrón-Quintana, P., Kuester, K., and Rubio-Ramírez, J. (2015). Fiscal volatility shocks and economic activity. *American Economic Review*, 105(11):3352–3384.

Ferrari, A. and Nispi Landi, V. (2024). Whatever it takes to save the planet? central banks and unconventional green policy. *Macroeconomic Dynamics*, 28(2):299–324.

Ferriani, F., Gazzani, A. G., and Natoli, F. (2024). The macroeconomic effects of green technology shocks. *Available at SSRN 4787604*.

Fried, S., Novan, K., and Peterman, W. B. (2021). The macro effects of climate policy uncertainty. *Finance and Economics Discussion Series*, (2021-018).

Gavriilidis, K. (2021). Measuring climate policy uncertainty. *Available at SSRN 3847388*.

Gertler, M. and Karadi, P. (2011). A model of unconventional monetary policy. *Journal of Monetary Economics*, 58(1):17–34.

Gibson, J. and Heutel, G. (2023). Pollution and labor market search externalities over the business cycle. *Journal of Economic Dynamics and Control*, 151:104665.

Gilchrist, S., Sim, J. W., and Zakrajšek, E. (2014). Uncertainty, financial frictions, and investment dynamics. Technical report, National Bureau of Economic Research.

Giovanardi, F., Kaldorf, M., Radke, L., and Wicknig, F. (2023). The preferential treatment of green bonds. *Review of Economic Dynamics*, 51:657–676.

Hambel, C., Kraft, H., and Schwartz, E. (2021). Optimal carbon abatement in a stochastic equilibrium model with climate change. *European Economic Review*, 132:103642.

Heutel, G. (2012). How should environmental policy respond to business cycles? optimal policy under persistent productivity shocks. *Review of Economic Dynamics*, 15(2):244–264.

Huang, B. and Punzi, M. T. (2024). Macroeconomic impact of environmental policy uncertainty and monetary policy implications. *Journal of Climate Finance*, 7:100040.

Jordà, (2005). Estimation and inference of impulse responses by local projections. *American Economic Review*, 95(1):161–182.

Jurado, K., Ludvigson, S. C., and Ng, S. (2015). Measuring uncertainty. *American Economic Review*, 105(3):1177–1216.

Khalil, M. and Strobel, F. (2023). *Capital reallocation under climate policy uncertainty*. Number 23/2023. Deutsche Bundesbank Discussion Paper.

Monasterolo, I., Mandel, A., Battiston, S., Mazzocchetti, A., Oppermann, K., Coony, J., Stretton, S., Stewart, F., and Dunz, N. (2024). The role of green financial sector initiatives in the low-carbon transition: A theory of change. *Global Environmental Change*, 89:102915.

NGFS (2024). Climate change, the macroeconomy and monetary policy. Technical report, Network for Greening the Financial System.

Noailly, J., Nowzohour, L., and Van Den Heuvel, M. (2022). Does environmental policy uncertainty hinder investments towards a low-carbon economy?

Noailly, J., Nowzohour, L., Van Den Heuvel, M., and Pla, I. (2024). Heard the news? environmental policy and clean investments. *Journal of Public Economics*, 238:105190.

Nordhaus, W. (2008). *A question of balance: Weighing the options on global warming policies*. Yale University Press.

Nordhaus, W. D. (2017). Revisiting the social cost of carbon. *Proceedings of the National Academy of Sciences*, 114(7):1518–1523.

Olea, J. L. M., Plagborg-Møller, M., Qian, E., and Wolf, C. K. (2025). Local projections or vars? a primer for macroeconomists.

Palikhe, H., Schaur, G., and Sims, C. (2024). Environmental policy uncertainty. *Journal of the Association of Environmental and Resource Economists*, 11(5):1135–1163.

Philip, K. (2024). Measuring swedish climate policy uncertainty and its impact on green bond credit spreads.

Pindyck, R. S. (1986). Irreversible investment, capacity choice, and the value of the firm.

Plagborg-Møller, M. and Wolf, C. K. (2021). Local projections and vars estimate the same impulse responses. *Econometrica*, 89(2):955–980.

Ramey, V. A. (2018). Ten years after the financial crisis: What have we learned from the vars? *Journal of Economic Perspectives*, 32(3):89–114.

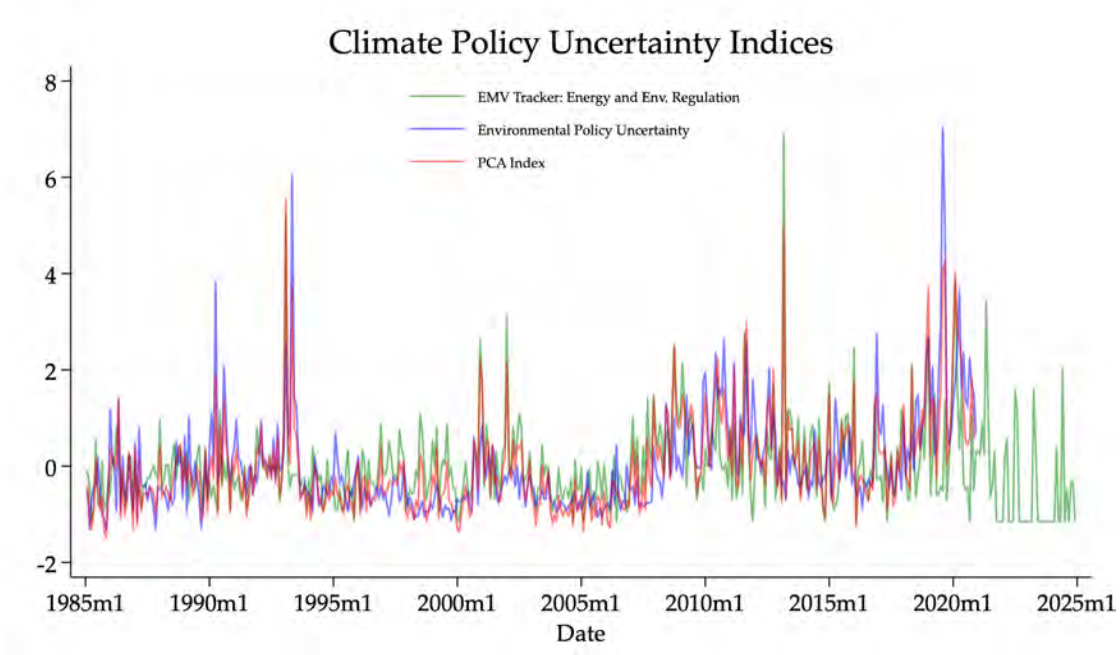
Ramey, V. A. and Zubairy, S. (2018). Government spending multipliers in good times and in bad: evidence from us historical data. *Journal of political economy*, 126(2):850–901.

Ren, X., Zhang, X., Yan, C., and Gozgor, G. (2022). Climate policy uncertainty and firm-level total factor productivity: Evidence from china. *Energy Economics*, 113:106209.

Rotemberg, J. J. (1982). Sticky prices in the united states. *Journal of Political Economy*, 90(6):1187–1211.

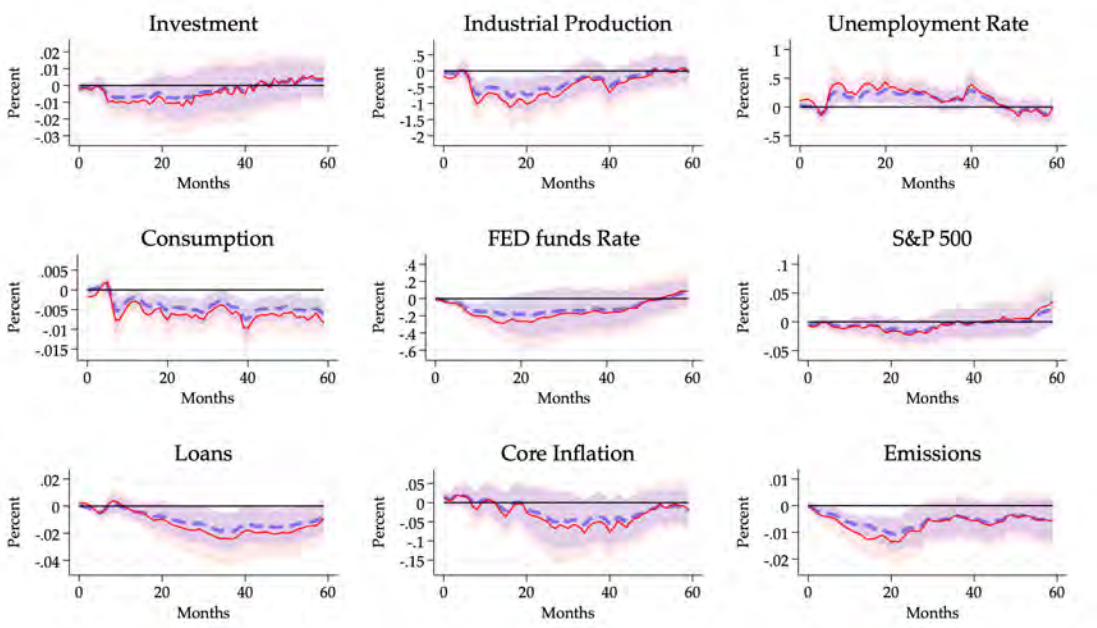
Tenreyro, S. and Thwaites, G. (2016). Pushing on a string: Us monetary policy is less powerful in recessions. *American Economic Journal: Macroeconomics*, 8(4):43–74.

## Appendix A.1: Climate Policy Uncertainty Indexes



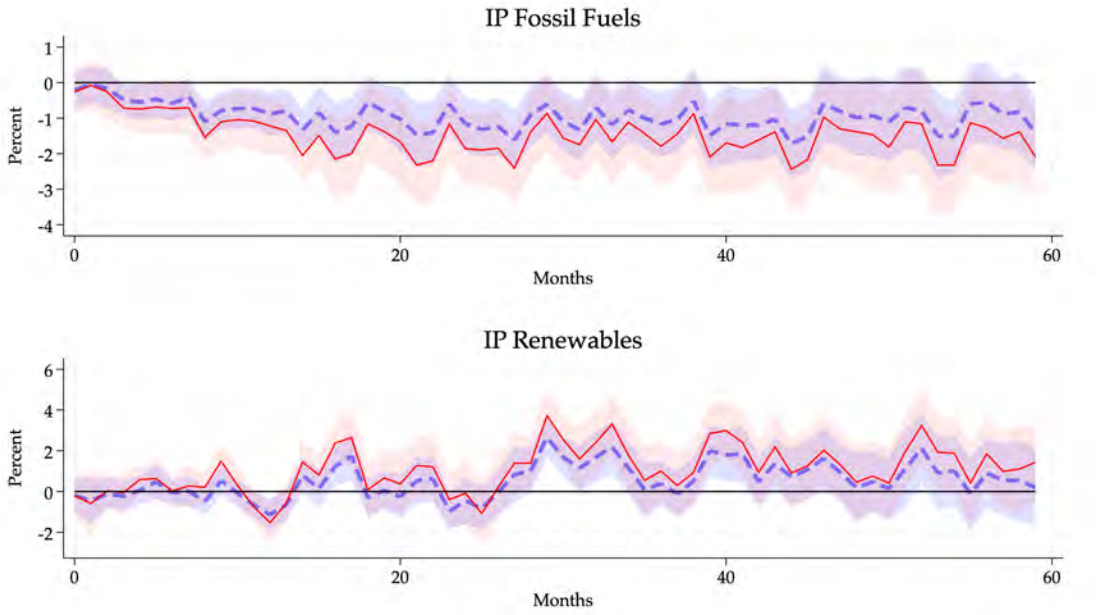
# Appendix A.2: Impulse Response Function to shock of the Individual Climate Policy Uncertainty Indices

**Figure 10:** Impulse Response Functions to 1 sd EnvPu Index - OLS (blue) and IV (red)



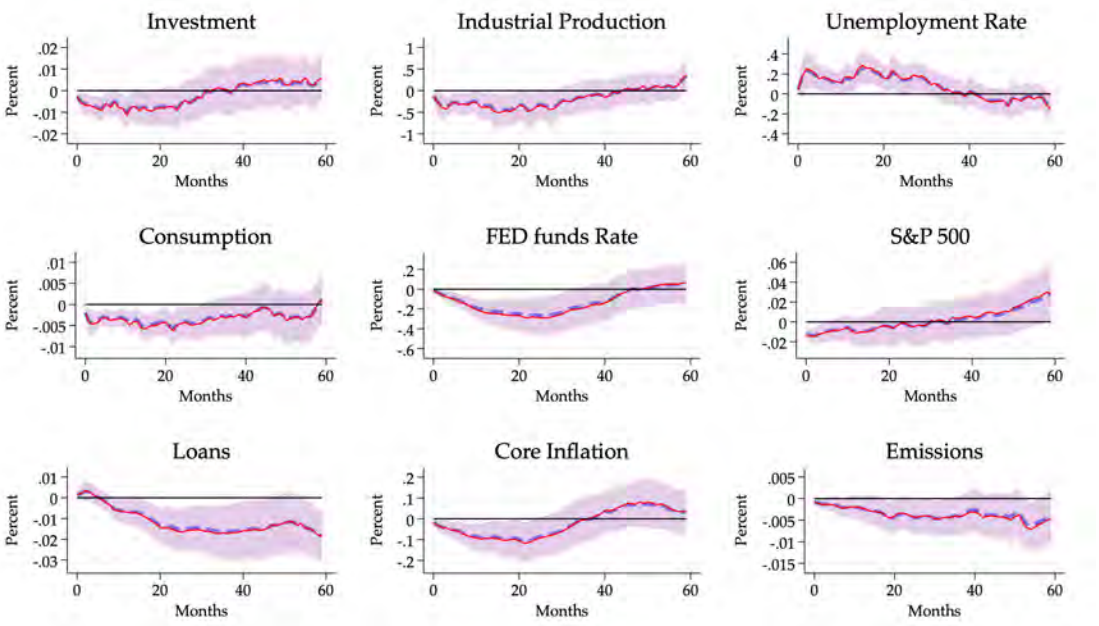

Note: 90% CI - In OLS I use the Index shock while in the IV the shock to instrument the index

**Figure 11:** Fossil Fuels and Low Carbon Energy IP to 1 sd EnvPu Index - OLS (blue) and IV (red)



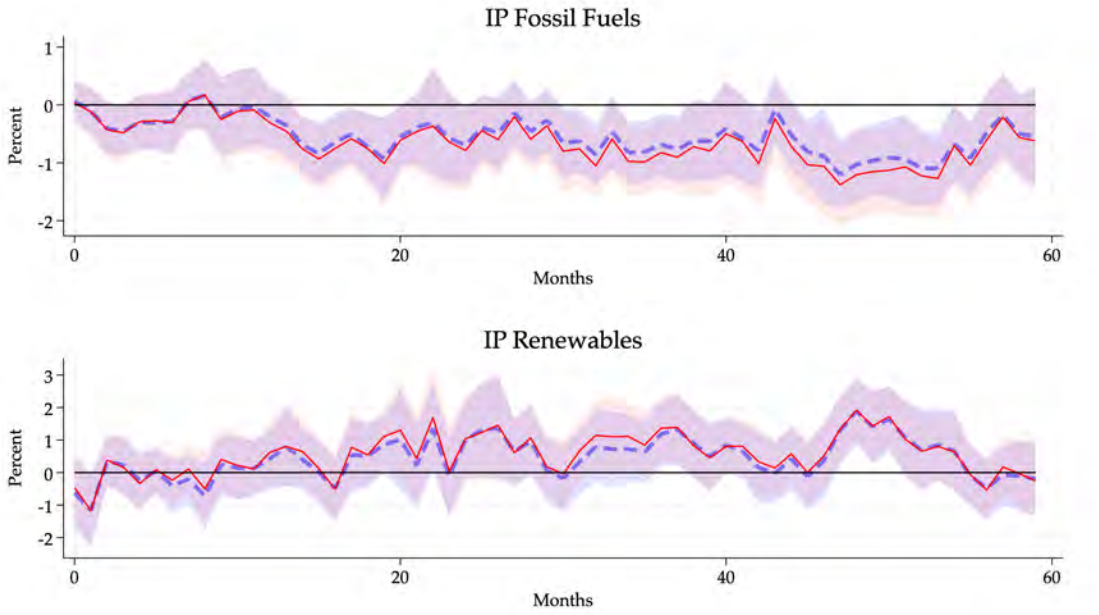

Note: 90% CI - In OLS I use the Index shock while in the IV the shock to instrument the index

**Figure 12:** Impulse Response Functions to 1 sd EMV-EER Index - OLS (blue) and IV (red)




Note: 90% CI - In OLS I use the Index shock while in the IV the shock to instrument the index

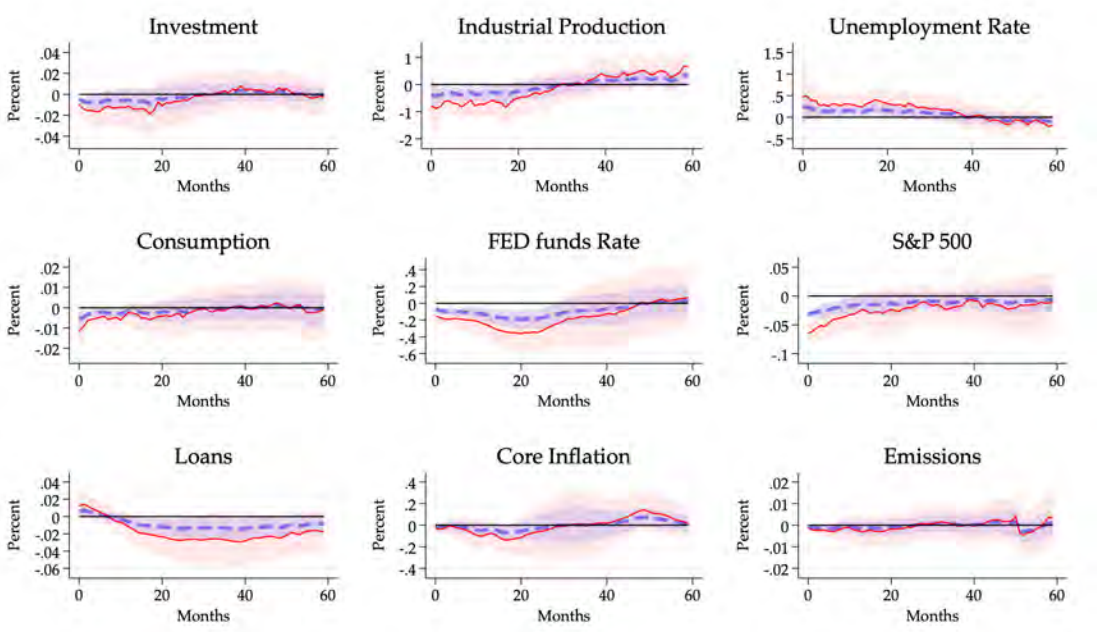
**Figure 13:** Fossil Fuels and Low Carbon Energy IP IRF to 1 sd EMV-EER Index - OLS (blue) and IV (red)




Note: 90% CI - In OLS I use the Index shock while in the IV the shock to instrument the index

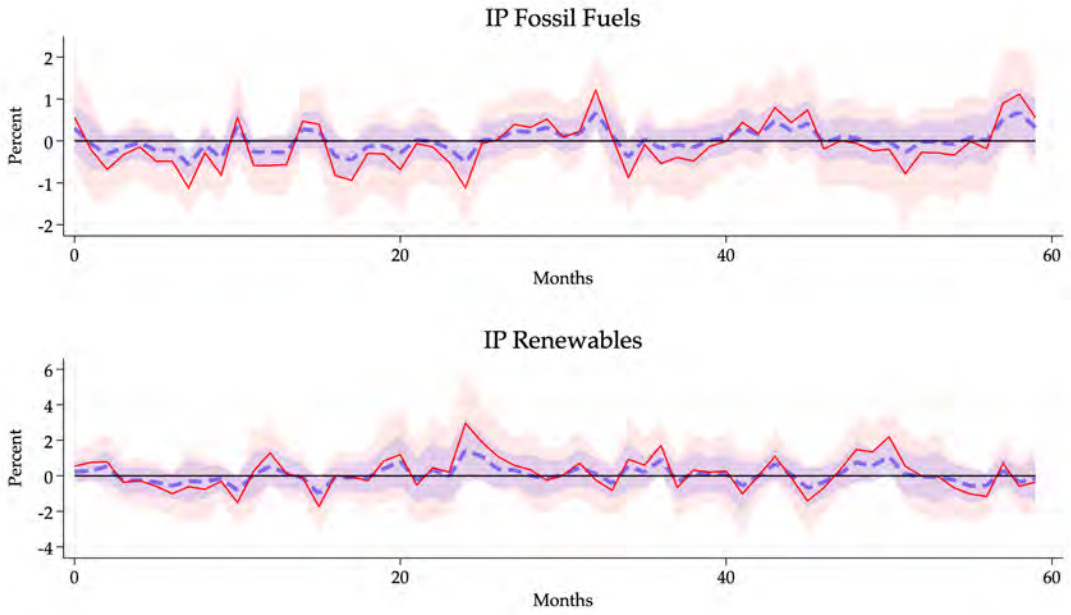
# Appendix A.3: Impulse Response Functions to traditional Uncertainty Measures - VIX and US EPU

**Figure 14:** Impulse Response Functions to 1 sd VIX- OLS (blue) and IV (red)



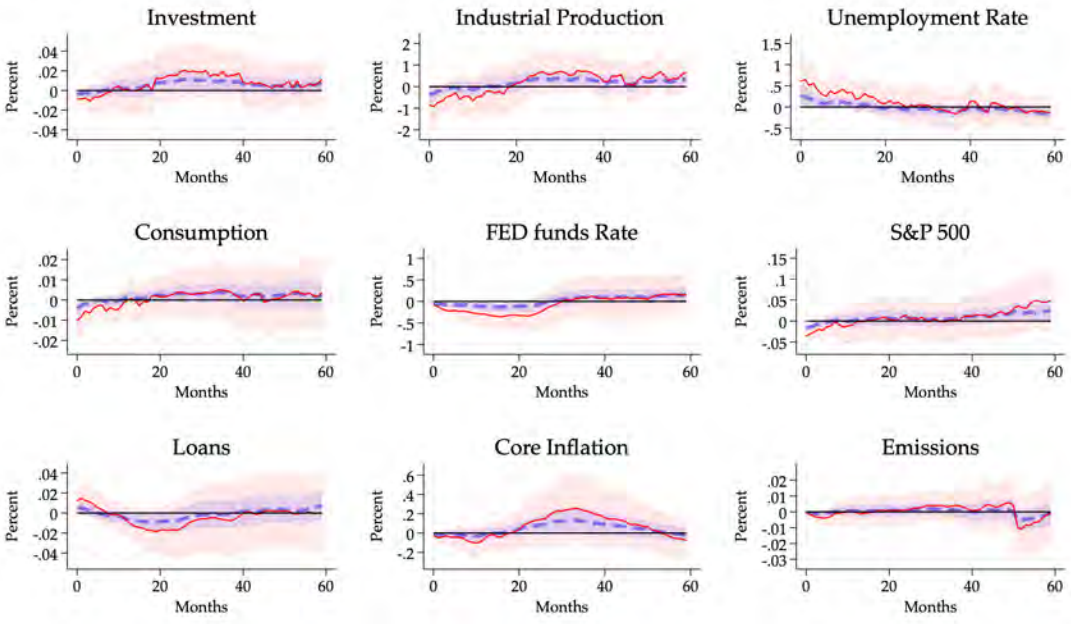

Note: 90% CI - In OLS I use the Index shock while in the IV the shock to instrument the index

**Figure 15:** Fossil Fuels and Low Carbon Energy IP- IRF to 1 sd VIX - OLS (blue) and IV (red)



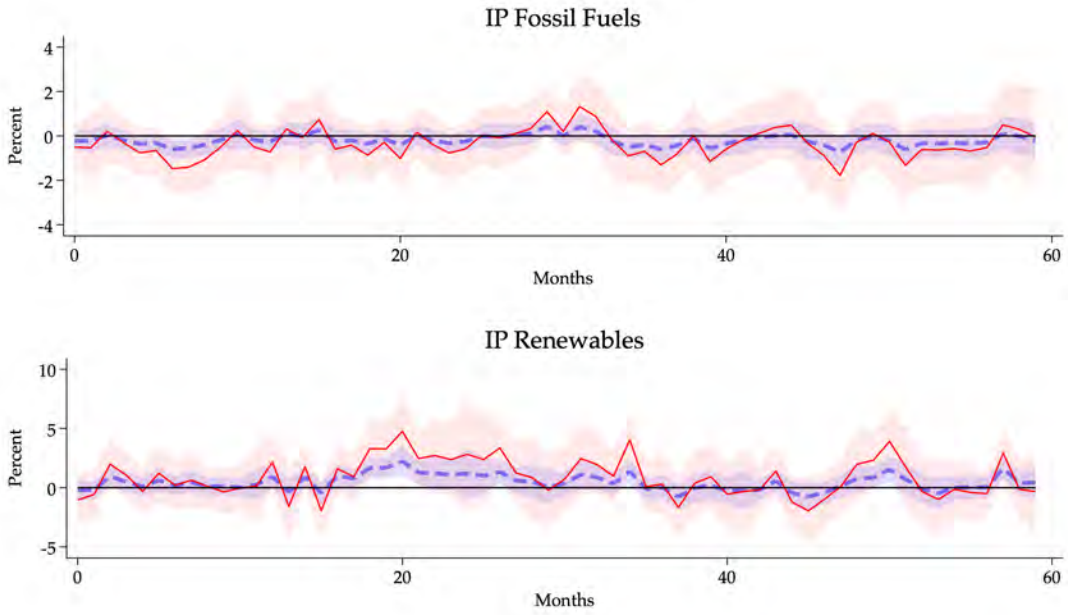

Note: 90% CI - In OLS I use the Index shock while in the IV the shock to instrument the index

**Figure 16:** Impulse Response Functions to 1 sd US EPU- OLS (blue) and IV (red)




Note: 90% CI - In OLS I use the Index shock while in the IV the shock to instrument the index

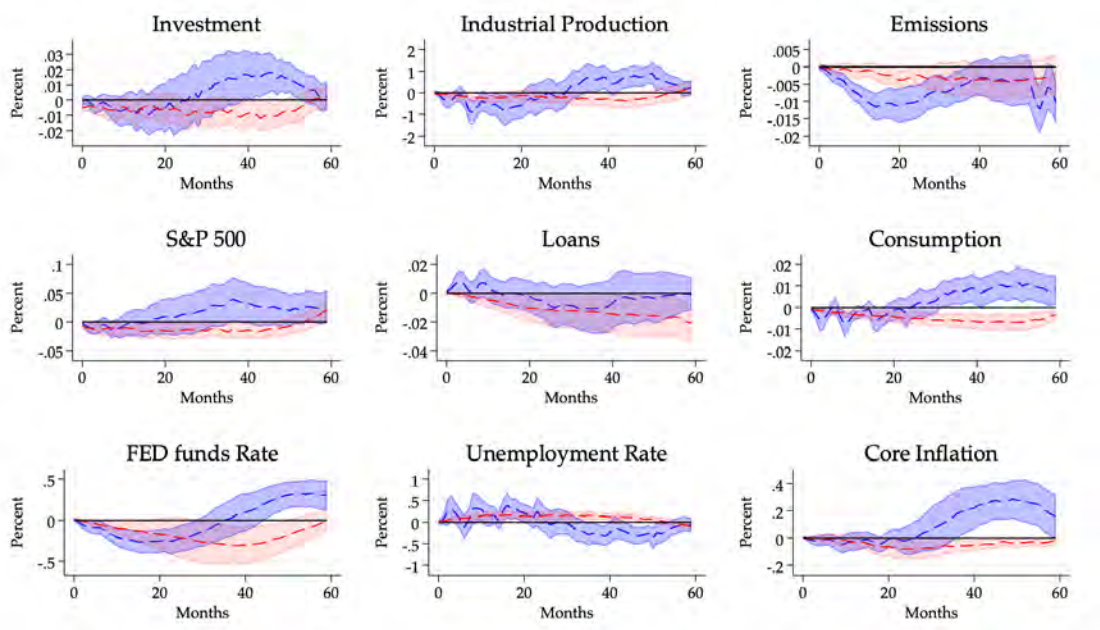
**Figure 17:** Fossil Fuels and Low Carbon Energy IP- IRF to 1 sd VIX - OLS (blue) and IV (red)




Note: 90% CI - In OLS I use the Index shock while in the IV the shock to instrument the index

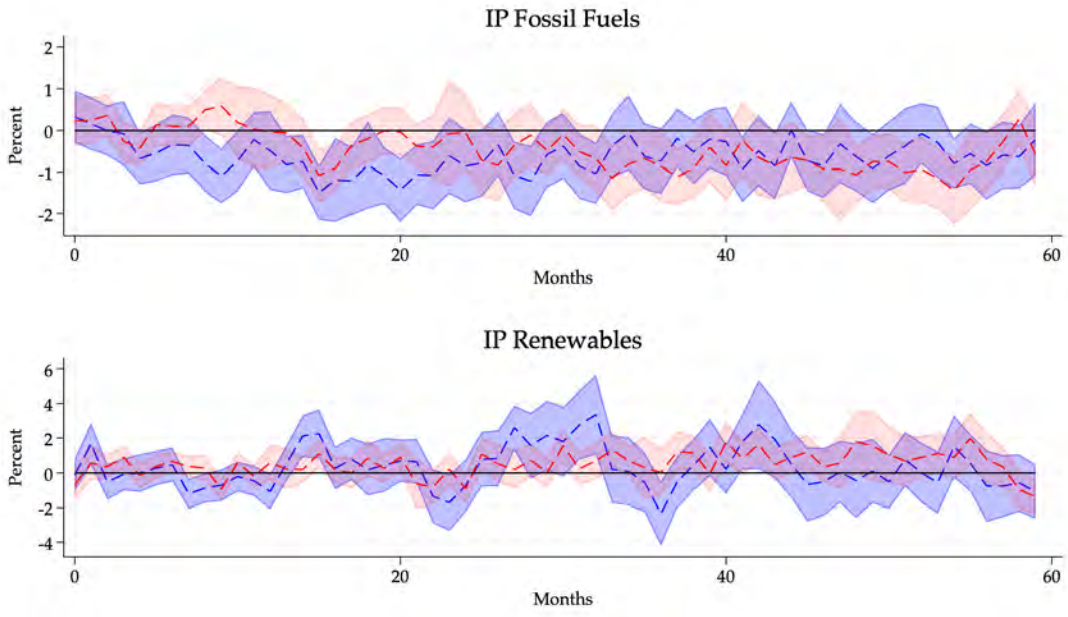
# Appendix A.4: State-Dependent Impulse Response Function Alternative Cutoff of Unemployment

**Figure 18:** OLS State Dependent IRF to 1 sd CPU PCA shock - Unemployment cutoff 5.5%



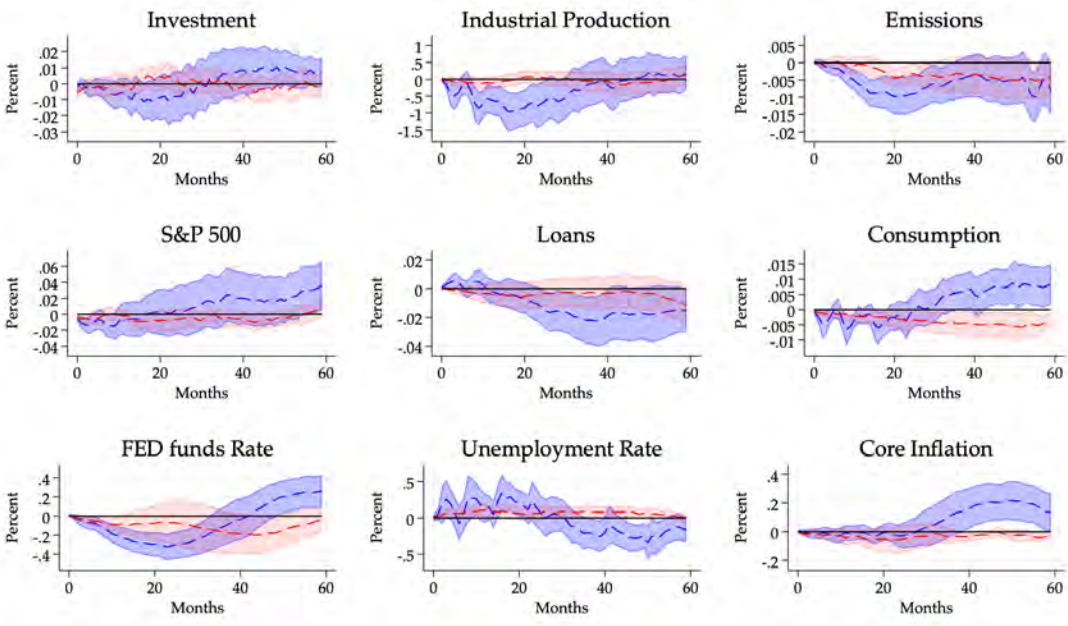

Note: 90% CI - High (red) vs Low (blue) Unemployment

**Figure 19:** IP Fossil and Renewable - OLS State Dependent IRF to 1 sd CPU PCA shock - Unemployment cutoff 5.5%



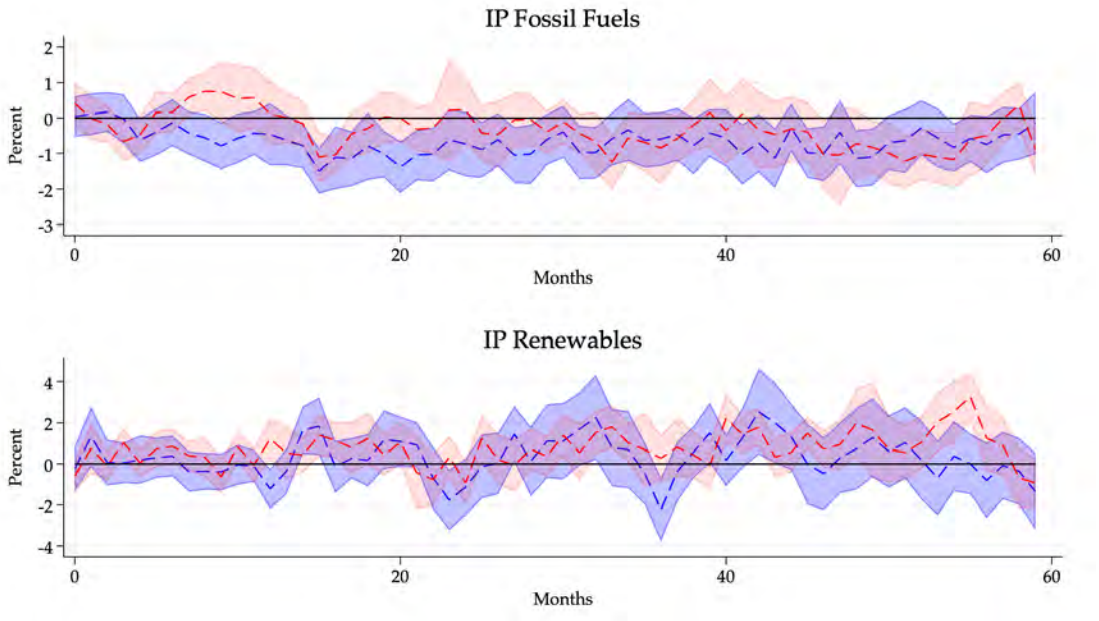

Note: 90% CI - High (red) vs Low (blue) Unemployment

**Figure 20:** OLS State Dependent IRF to 1 sd CPU PCA shock - Unemployment cutoff 6%



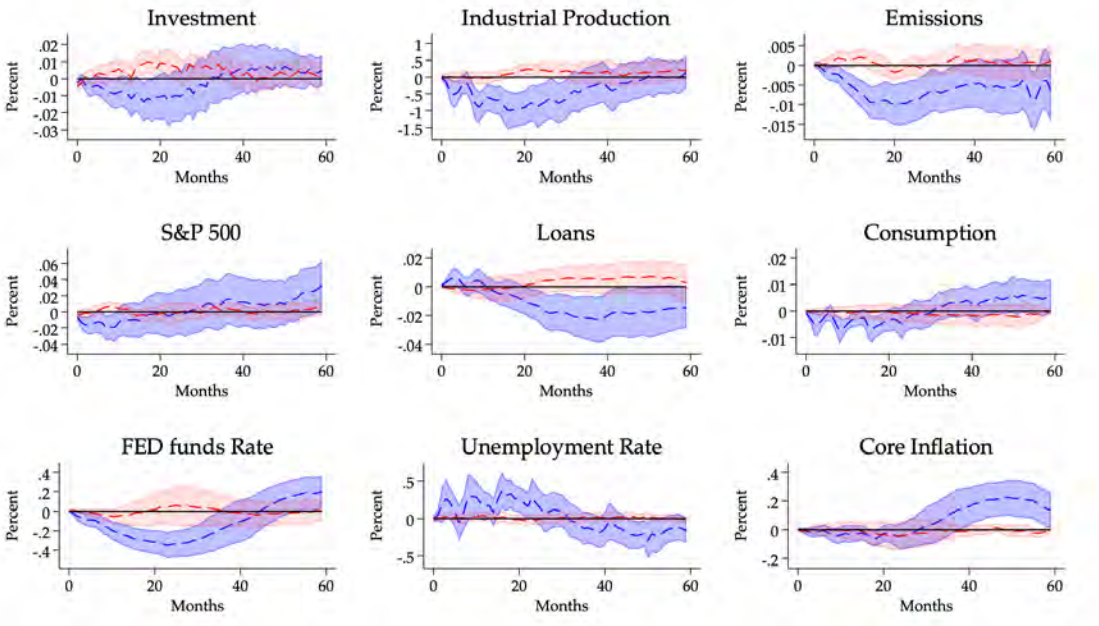

Note: 90% CI - High (red) vs Low (blue) Unemployment

**Figure 21:** IP Fossil and Renewable - OLS State Dependent IRF to 1 sd CPU PCA shock - Unemployment cutoff 6%



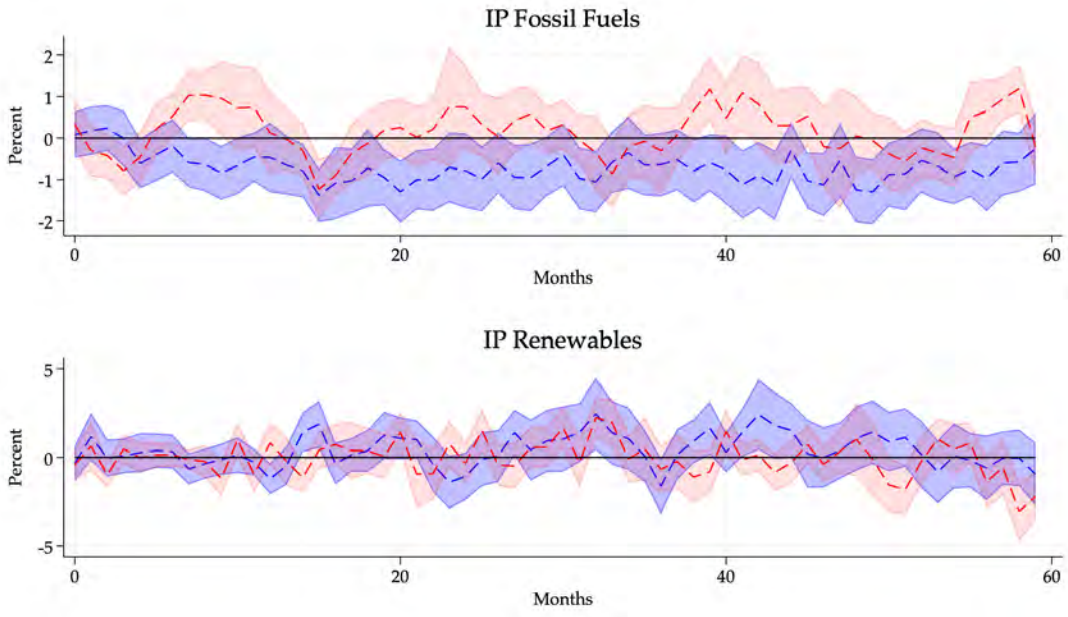

Note: 90% CI - High (red) vs Low (blue) Unemployment

**Figure 22:** OLS State Dependent IRF to 1 sd CPU PCA shock - Unemployment cutoff 6.5%



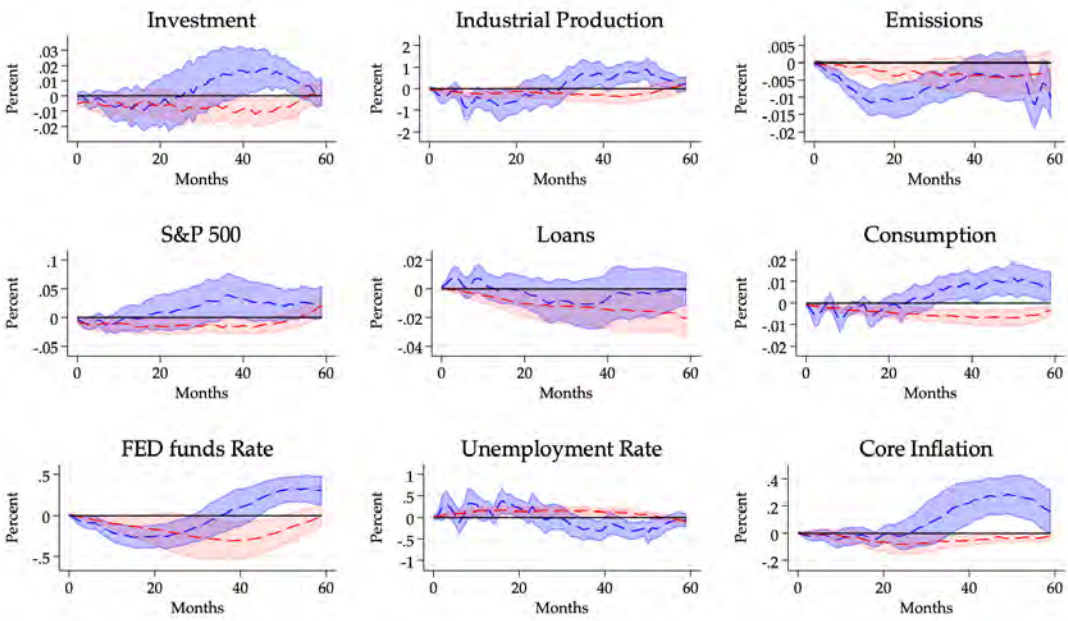

Note: 90% CI - High (red) vs Low (blue) Unemployment

**Figure 23:** IP Fossil and Renewable - OLS State Dependent IRF to 1 sd CPU PCA shock - Unemployment cutoff 6.5%



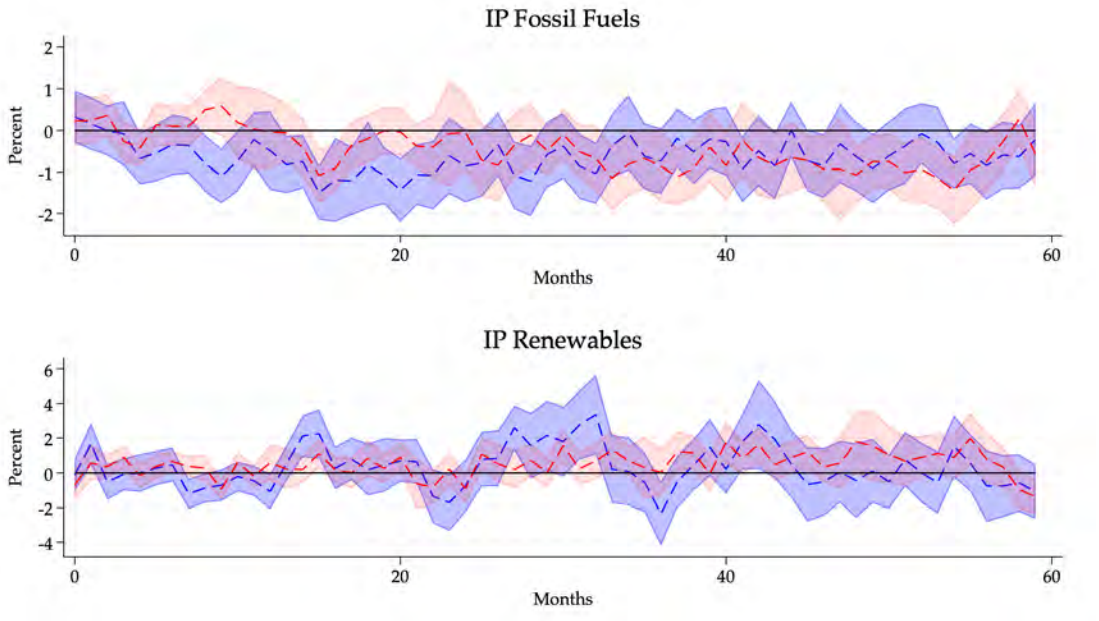

Note: 90% CI - High (red) vs Low (blue) Unemployment

**Figure 24:** OLS State Dependent IRF to 1 sd VIX shock - Unemployment cutoff 5.5%



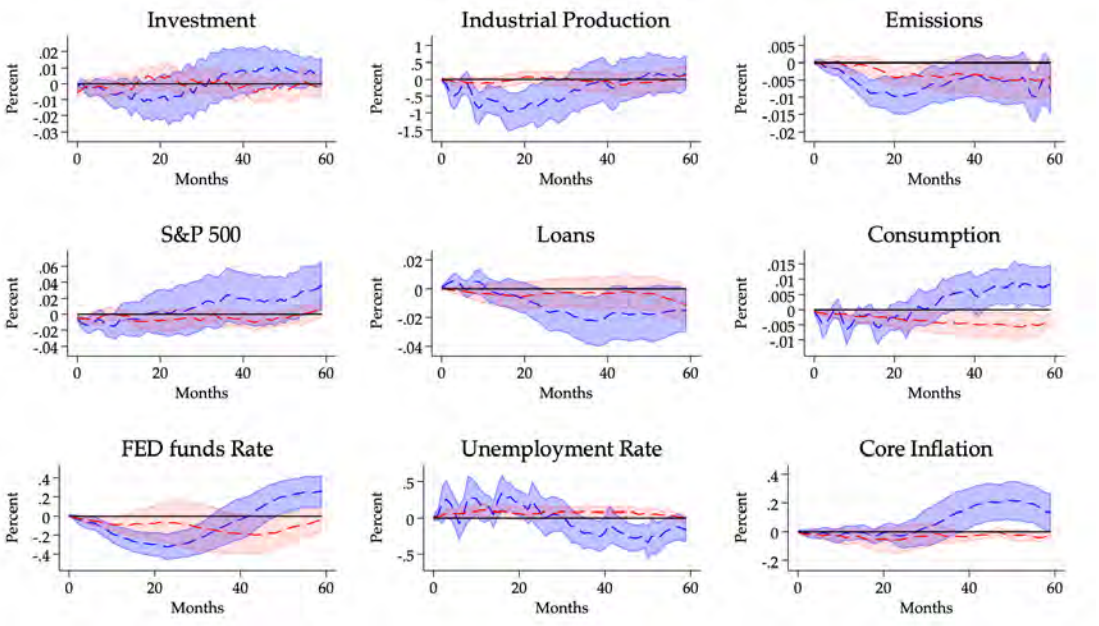

Note: 90% CI - High (red) vs Low (blue) Unemployment

**Figure 25:** IP Fossil and Renewable - OLS State Dependent IRF to 1 sd VIX shock - Unemployment cutoff 5.5%



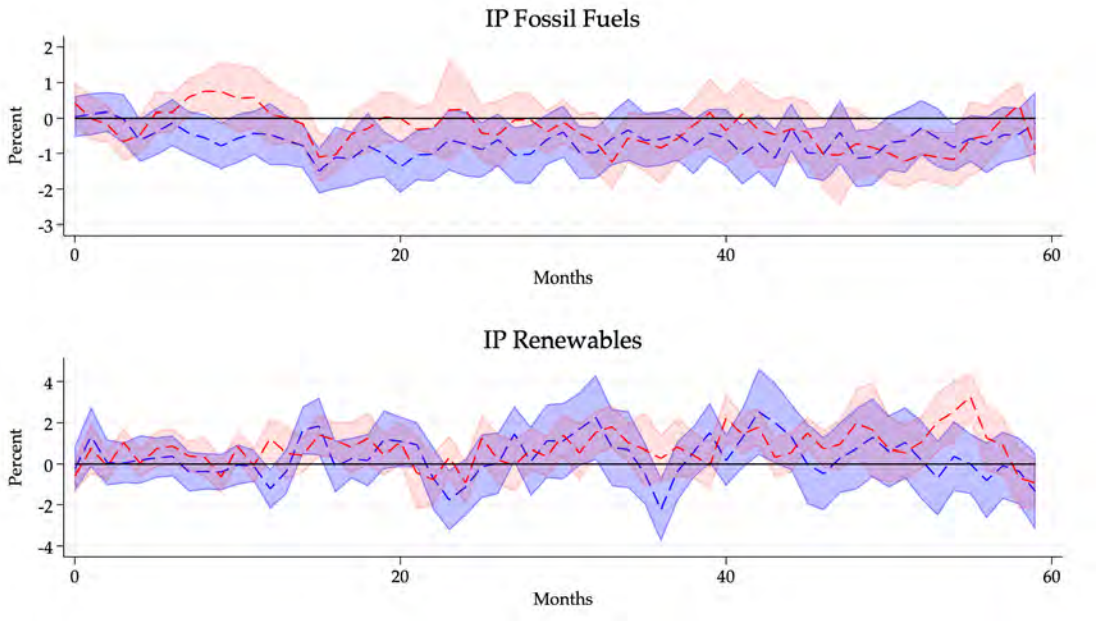

Note: 90% CI - High (red) vs Low (blue) Unemployment

**Figure 26:** OLS State Dependent IRF to 1 sd VIX shock - Unemployment cutoff 6%



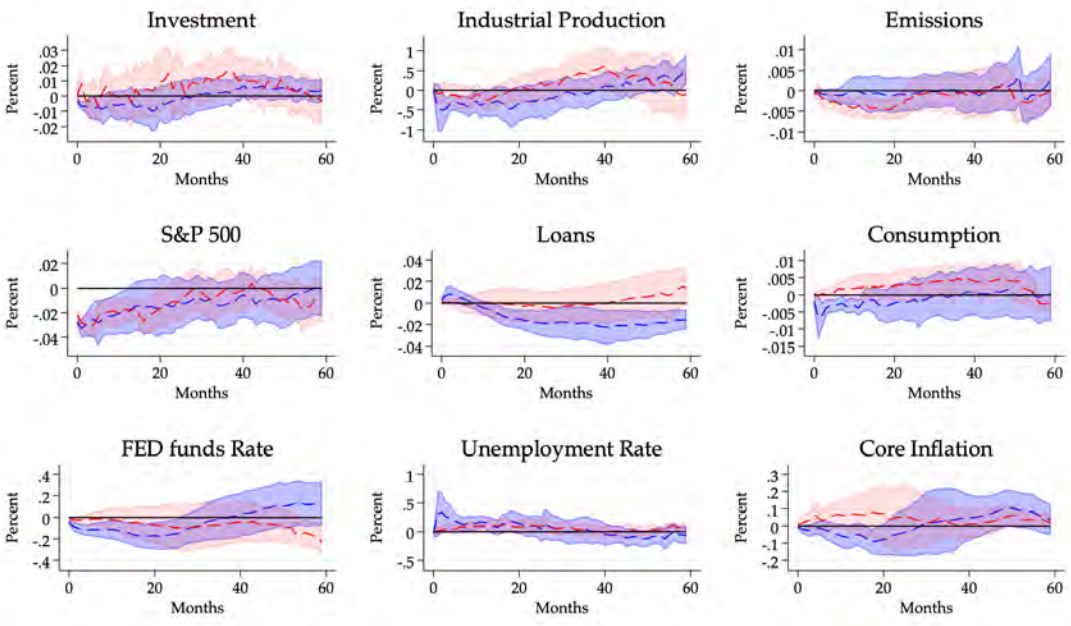

Note: 90% CI - High (red) vs Low (blue) Unemployment

**Figure 27:** IP Fossil and Renewable - OLS State Dependent IRF to 1 sd VIX shock - Unemployment cutoff 6%



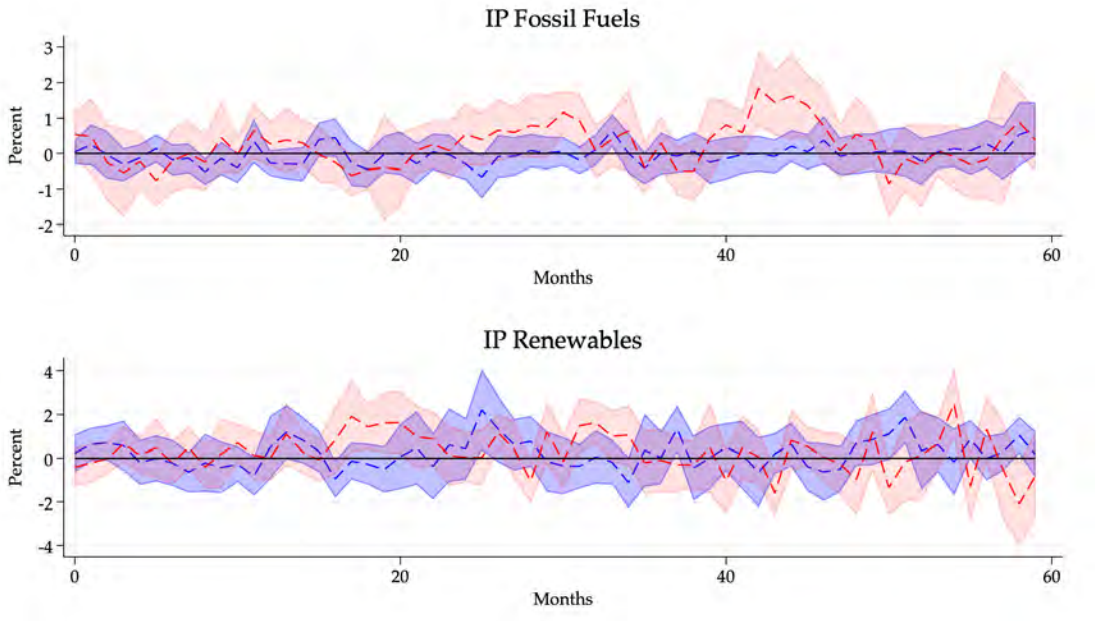

Note: 90% CI - High (red) vs Low (blue) Unemployment

**Figure 28:** OLS State Dependent IRF to 1 sd VIX shock - Unemployment cutoff 6.5%




Note: 90% CI - High (red) vs Low (blue) Unemployment

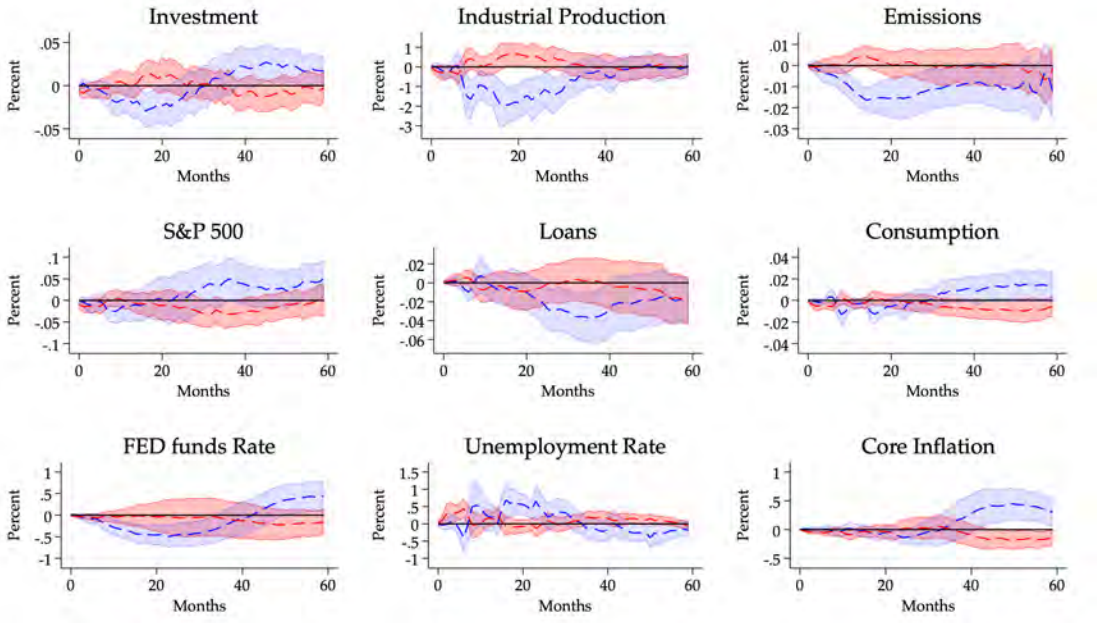
**Figure 29:** IP Fossil and Renewable - OLS State Dependent IRF to 1 sd VIX shock - Unemployment cutoff 6.5%




Note: 90% CI - High (red) vs Low (blue) Unemployment

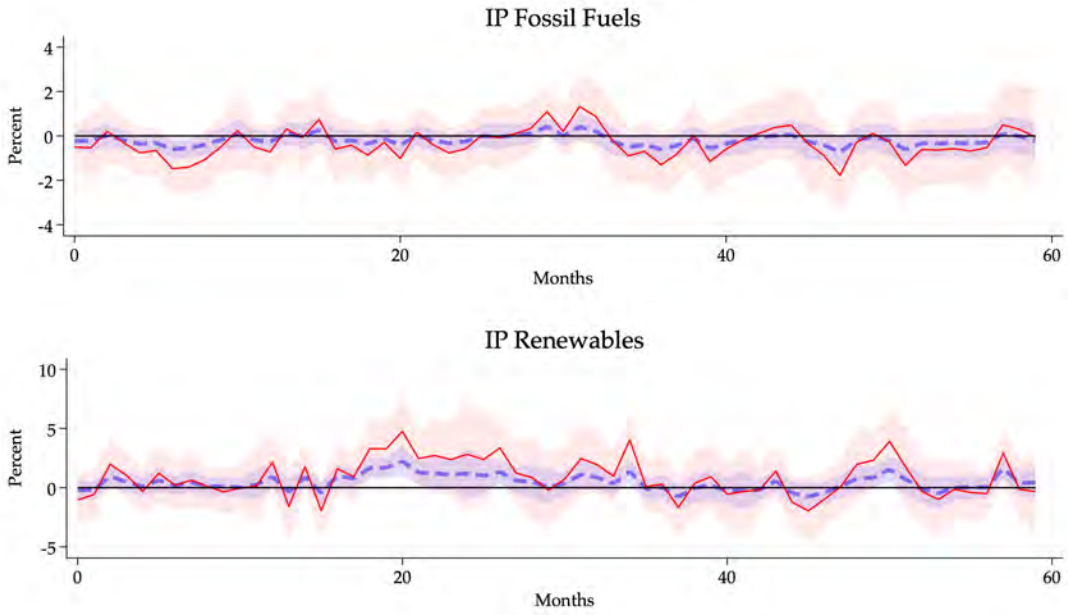
# Appendix A.5: State-Dependent Impulse Response Function - Auerbach and Gorodnichenko (2012) Methodology

**Figure 30:** OLS State Dependent IRF to 1 sd CPU PCA shock - $\gamma = 1$



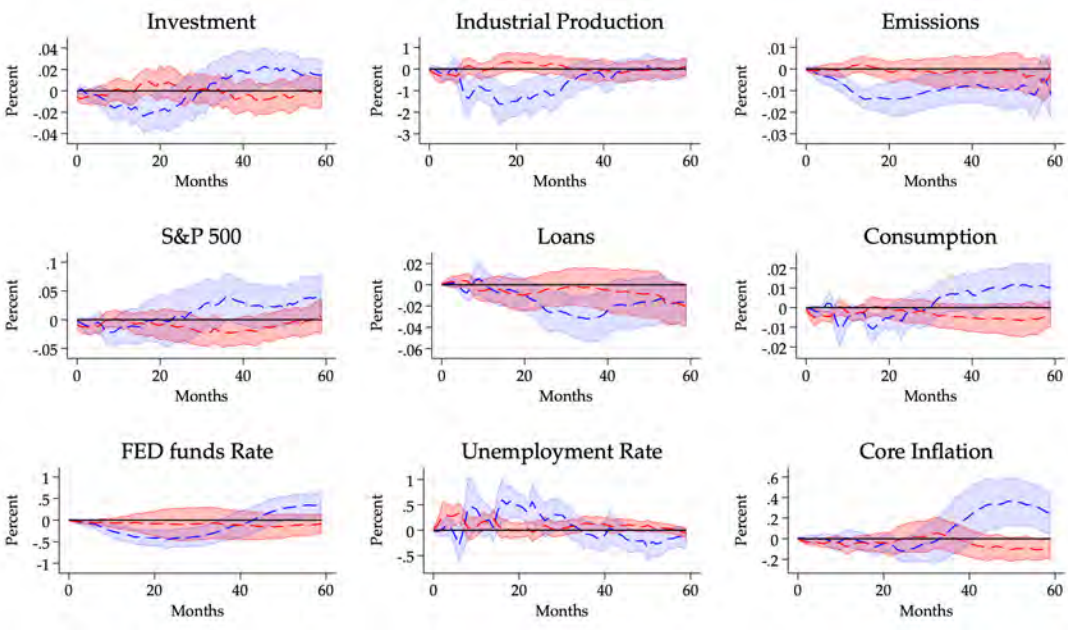

Note: 90% CI - High (red) vs Low (blue) Unemployment

**Figure 31:** IP Fossil and Renewable - OLS State Dependent IRF to 1 sd CPU PCA shock - $\gamma = 1$



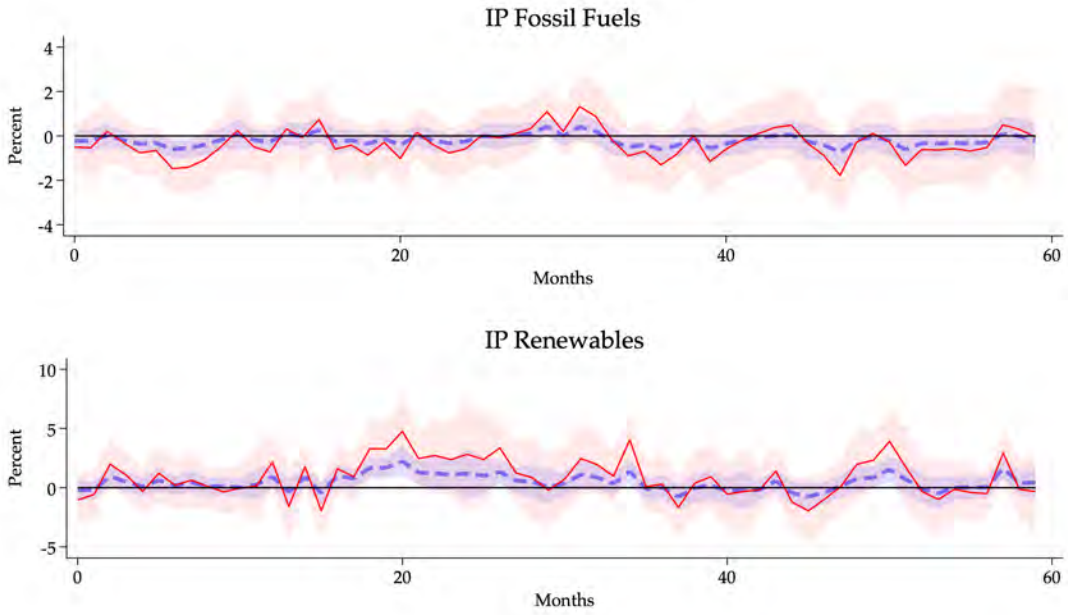

Note: 90% CI - High (red) vs Low (blue) Unemployment

**Figure 32:** OLS State Dependent IRF to 1 sd CPU PCA shock - $\gamma = 1.5$



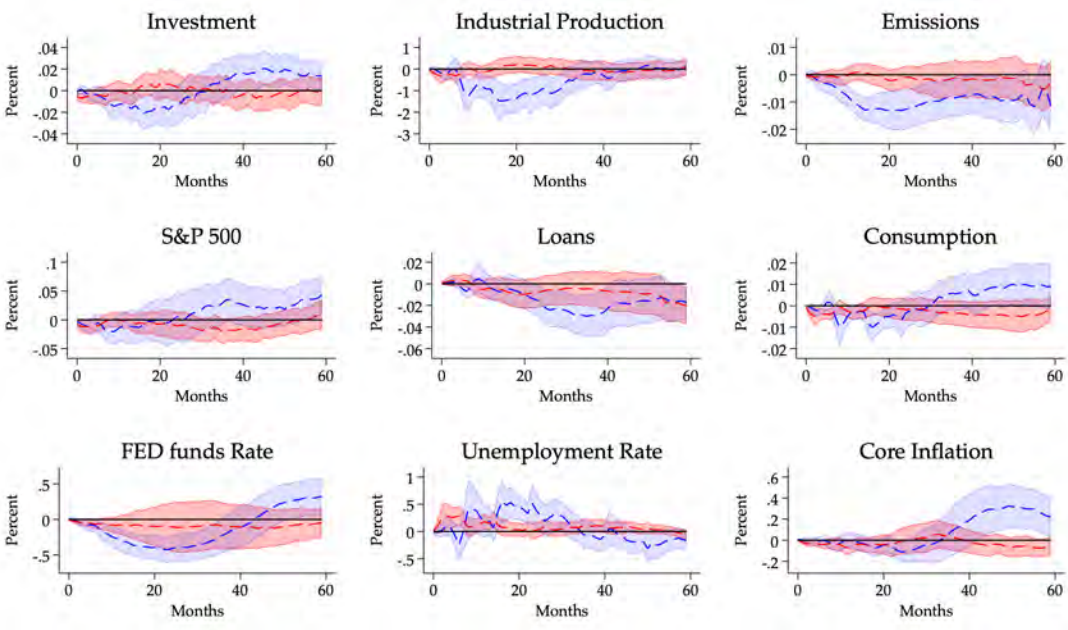

Note: 90% CI - High (red) vs Low (blue) Unemployment

**Figure 33:** IP Fossil and Renewable - OLS State Dependent IRF to 1 sd CPU PCA shock - $\gamma = 1.5$



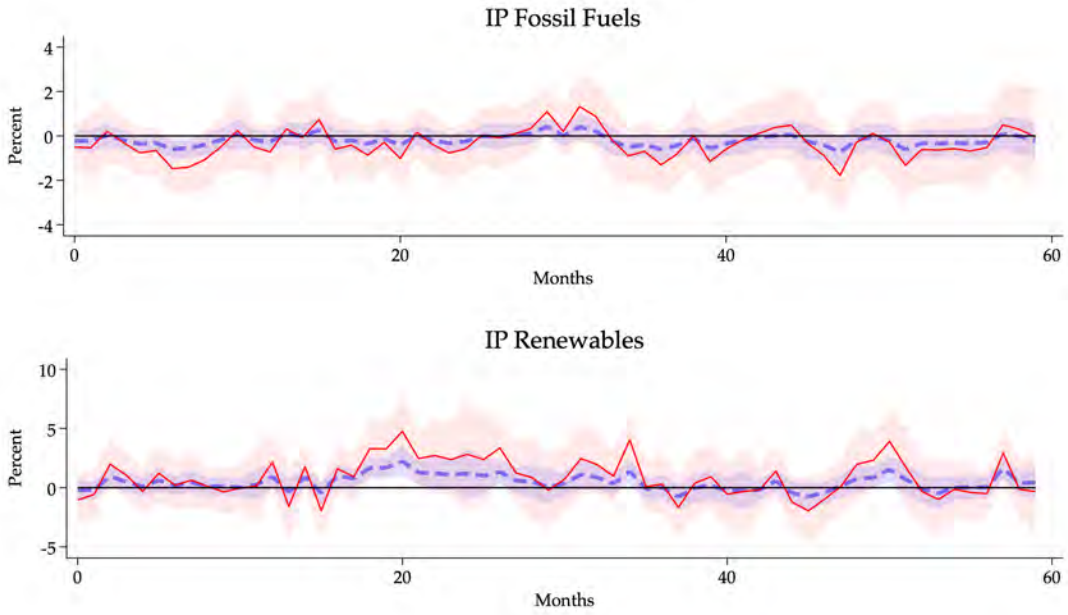

Note: 90% CI - High (red) vs Low (blue) Unemployment

**Figure 34:** OLS State Dependent IRF to 1 sd CPU PCA shock - $\gamma = 2$



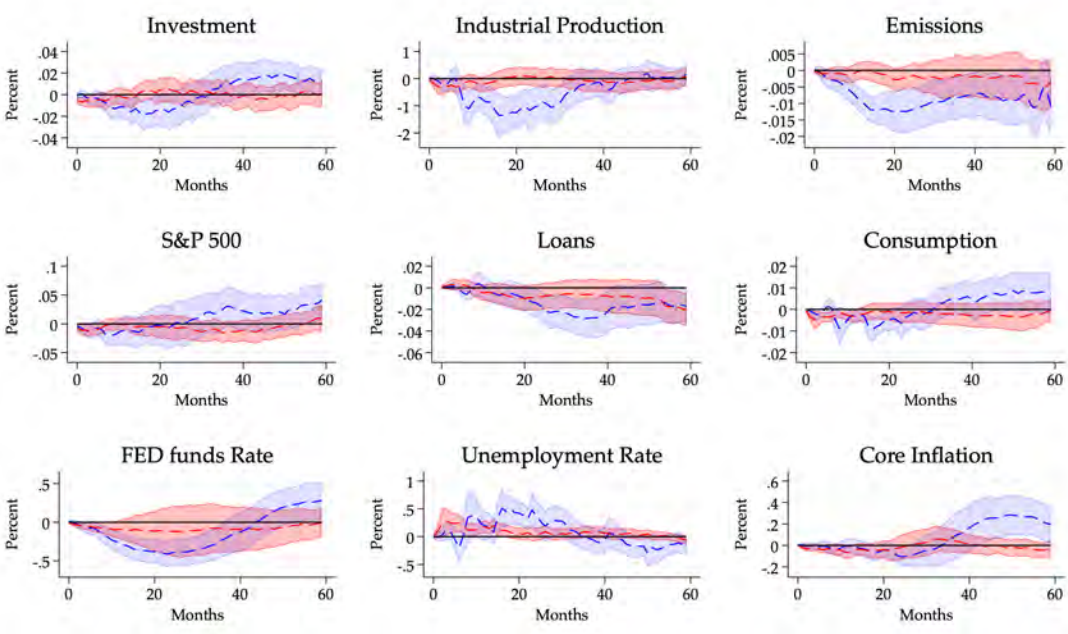

Note: 90% CI - High (red) vs Low (blue) Unemployment

**Figure 35:** IP Fossil and Renewable - OLS State Dependent IRF to 1 sd CPU PCA shock - $\gamma = 2$



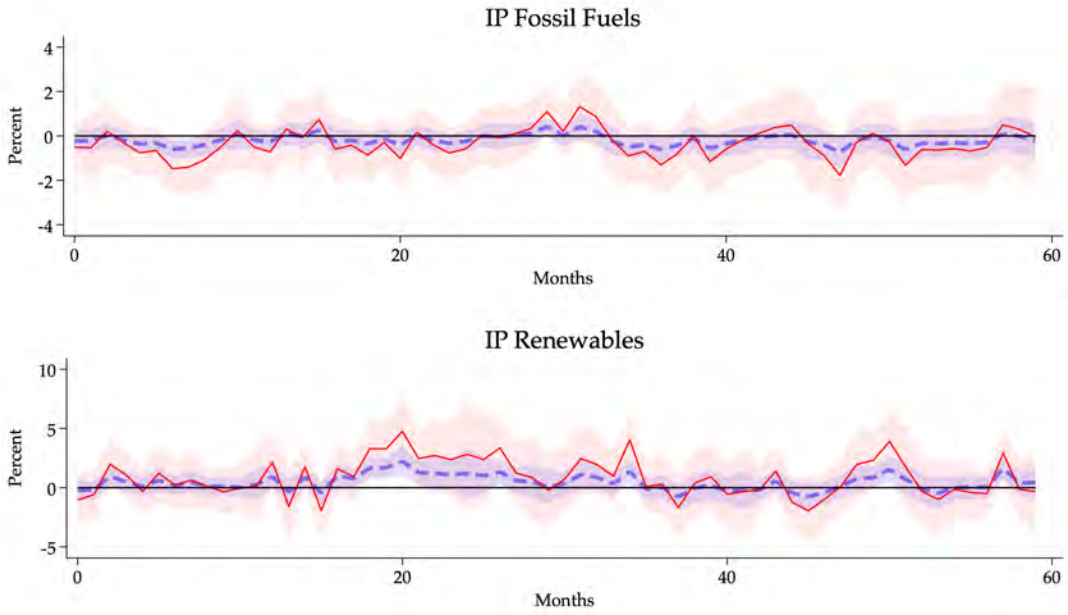

Note: 90% CI - High (red) vs Low (blue) Unemployment

**Figure 36:** OLS State Dependent IRF to 1 sd CPU PCA shock - $\gamma = 3$



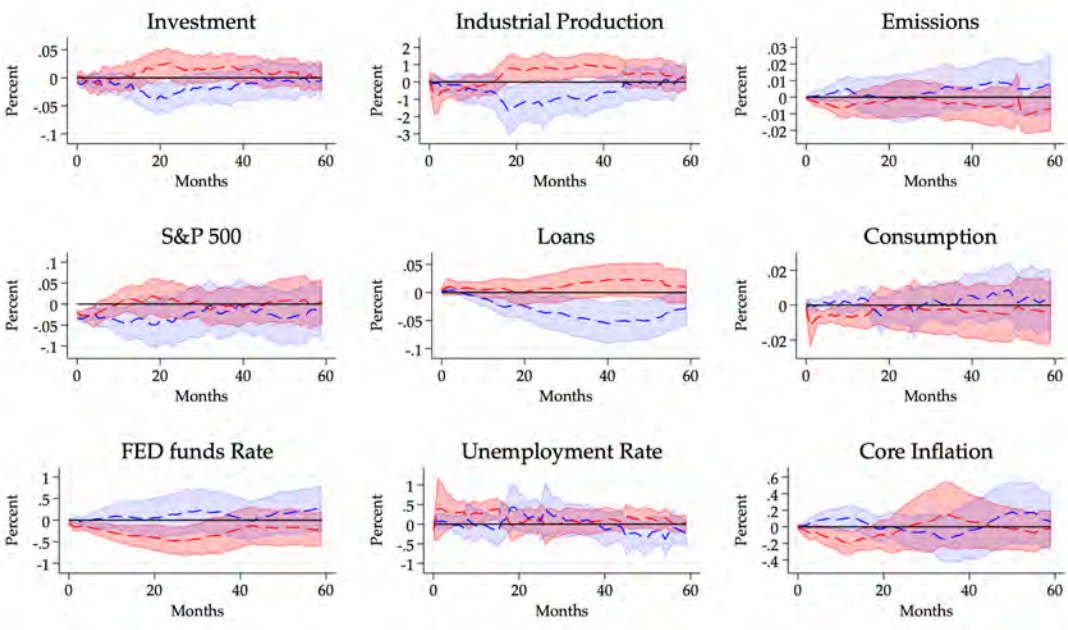

Note: 90% CI - High (red) vs Low (blue) Unemployment

**Figure 37:** IP Fossil and Renewable - OLS State Dependent IRF to 1 sd CPU PCA shock - $\gamma = 3$



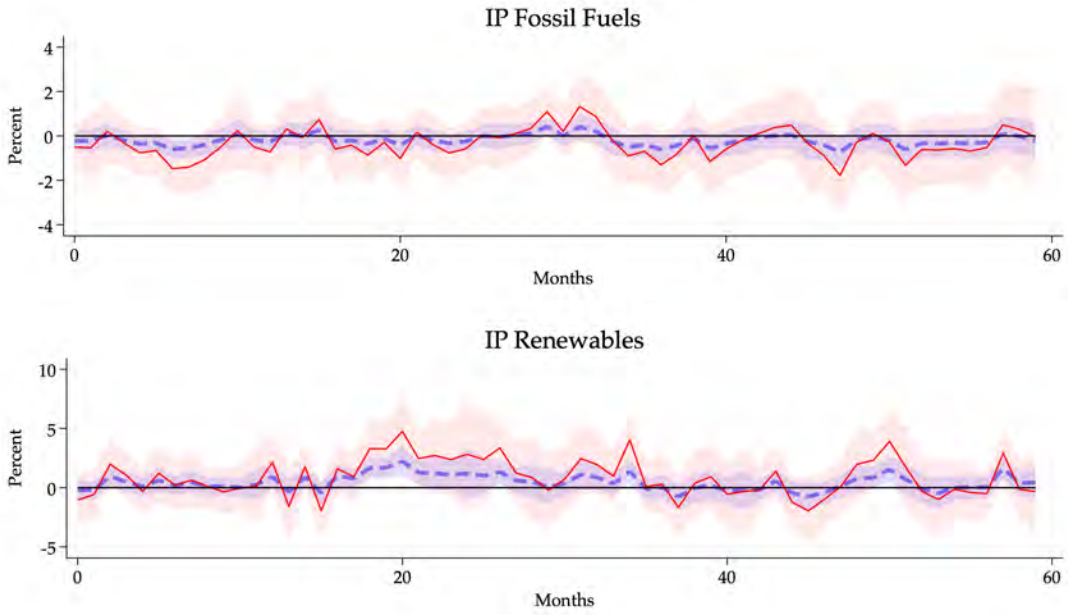

Note: 90% CI - High (red) vs Low (blue) Unemployment

**Figure 38:** OLS State Dependent IRF to 1 sd VIX shock - $\gamma = 1$



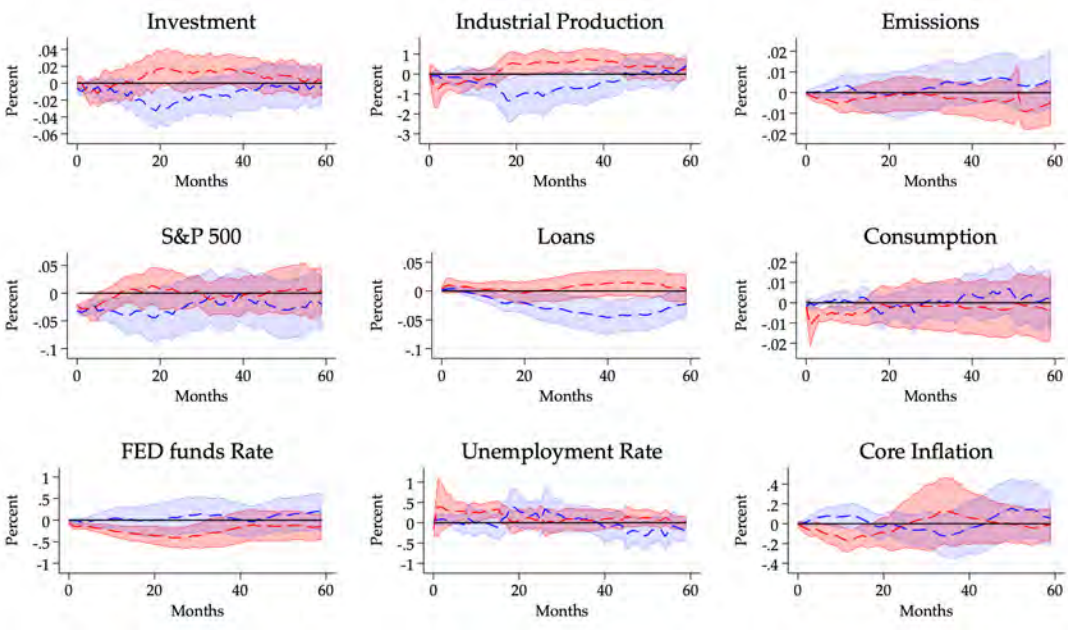

Note: 90% CI - High (red) vs Low (blue) Unemployment

**Figure 39:** IP Fossil and Renewable - OLS State Dependent IRF to 1 sd VIX shock - $\gamma = 1$



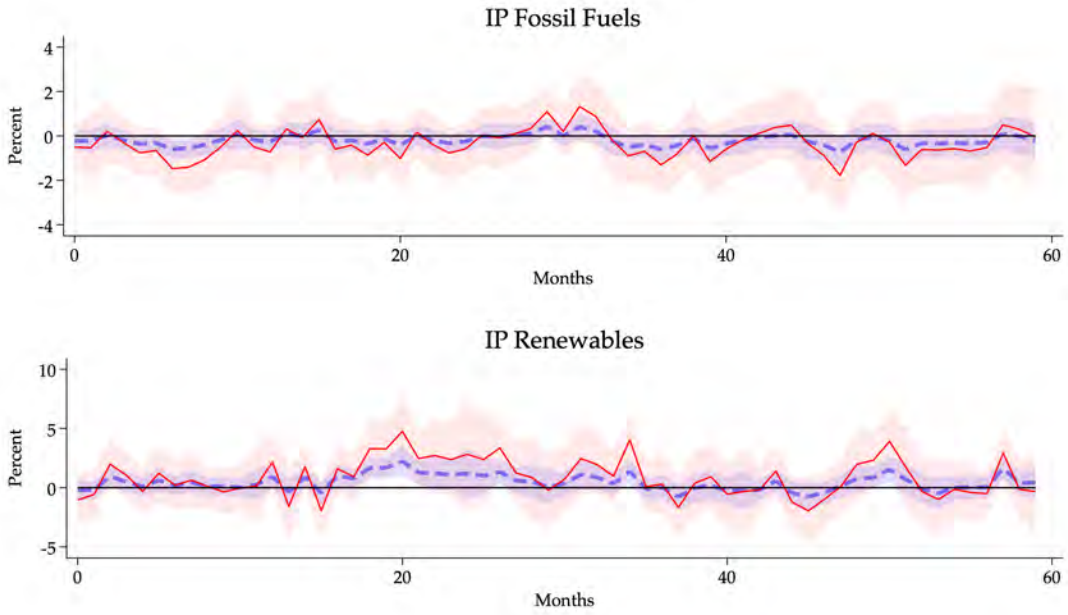

Note: 90% CI - High (red) vs Low (blue) Unemployment

**Figure 40:** OLS State Dependent IRF to 1 sd VIX shock - $\gamma = 1.5$



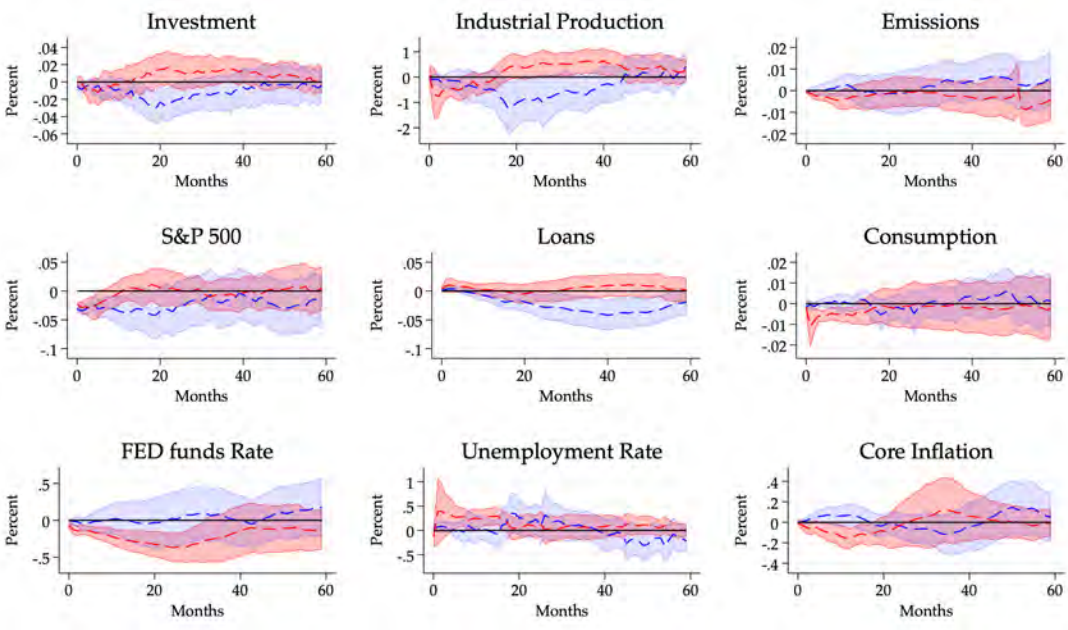

Note: 90% CI - High (red) vs Low (blue) Unemployment

**Figure 41:** IP Fossil and Renewable - OLS State Dependent IRF to 1 sd VIX shock - $\gamma = 1.5$



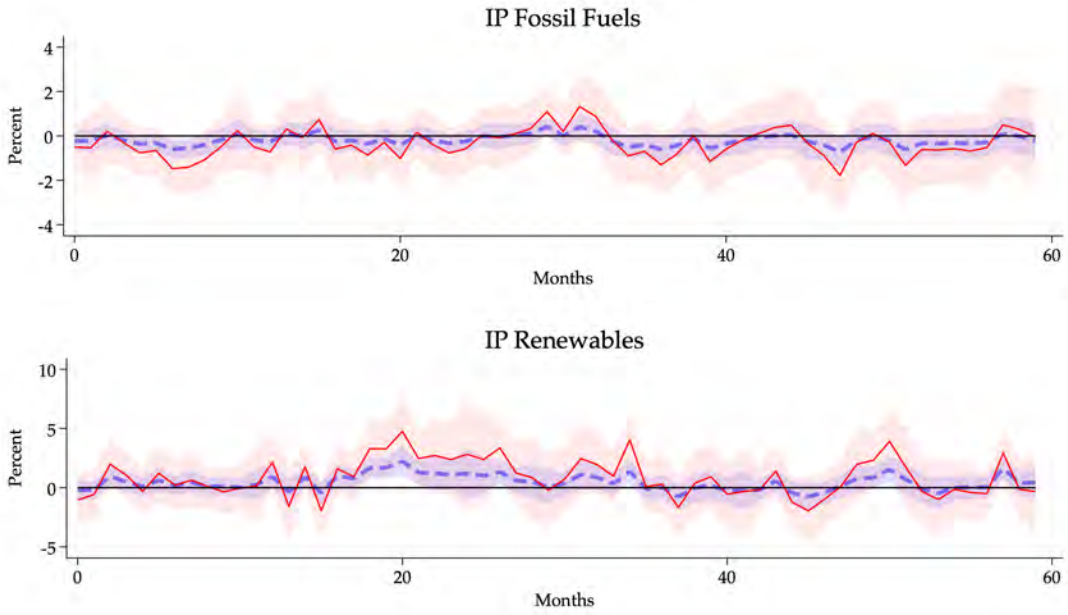

Note: 90% CI - High (red) vs Low (blue) Unemployment

**Figure 42:** OLS State Dependent IRF to 1 sd VIX shock - $\gamma = 2$



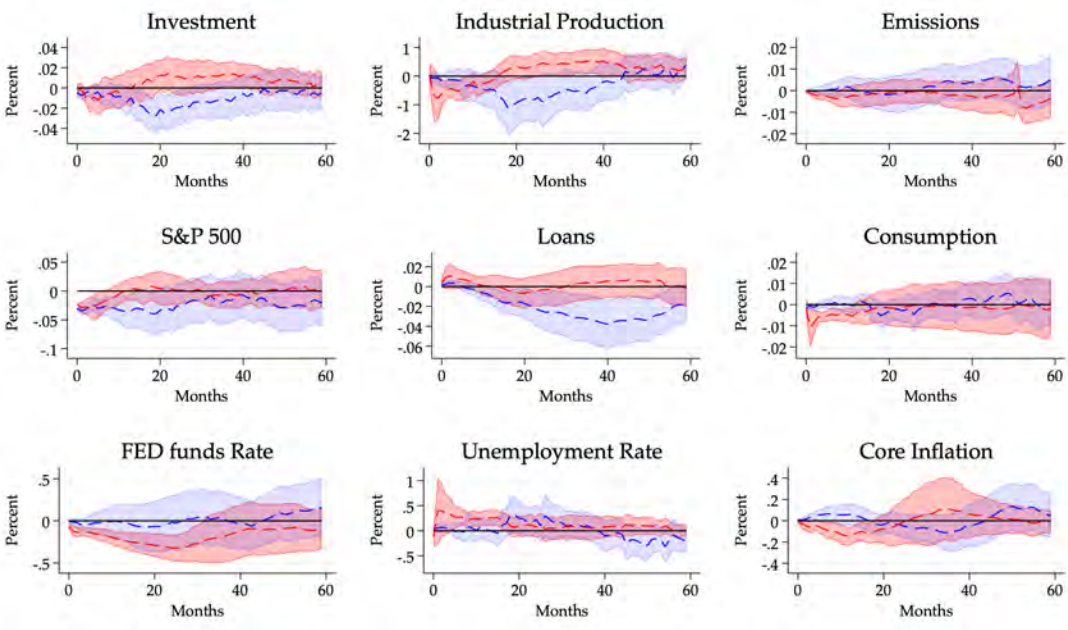

Note: 90% CI - High (red) vs Low (blue) Unemployment

**Figure 43:** IP Fossil and Renewable - OLS State Dependent IRF to 1 sd VIX shock - $\gamma = 2$



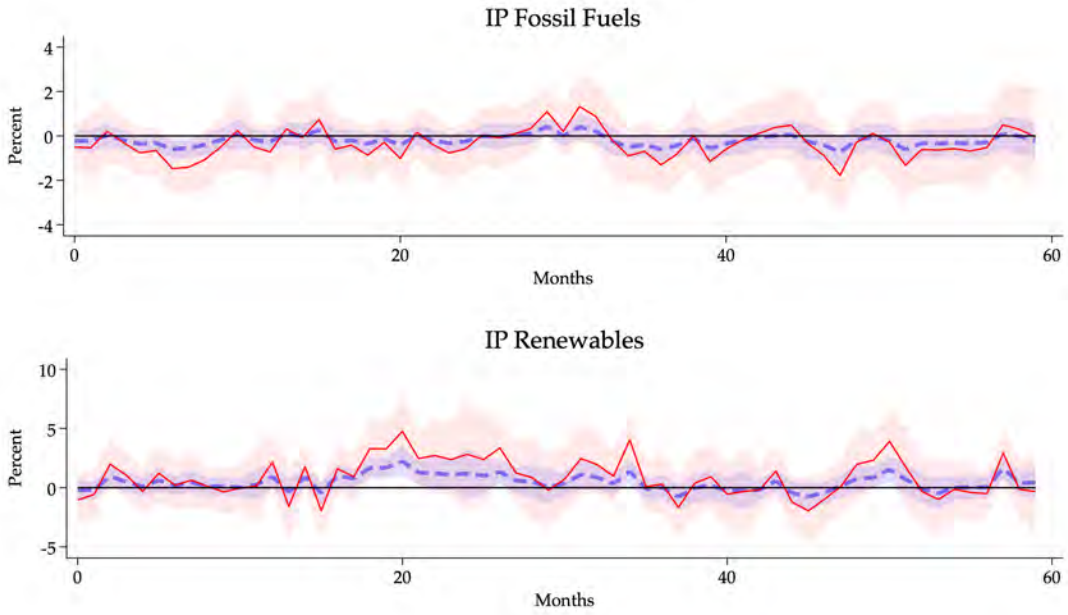

Note: 90% CI - High (red) vs Low (blue) Unemployment

**Figure 44:** OLS State Dependent IRF to 1 sd VIX shock - $\gamma = 3$




Note: 90% CI - High (red) vs Low (blue) Unemployment

**Figure 45:** IP Fossil and Renewable - OLS State Dependent IRF to 1 sd VIX shock - $\gamma = 3$




Note: 90% CI - High (red) vs Low (blue) Unemployment

## Appendix B: Calibrated Parameters

We follow Ferrari and Nispi Landi (2024) and calibrate ex-ante the parameters:

- $Lev = 6$
- $\frac{\bar{r}}{pi} = R = 1.05$
- $RoW = \frac{e^{row}}{e} = 15.3$
- $\frac{k^G}{k} = 0.2$
- $\frac{g}{y} = 0.215$
- $\frac{b^P}{4y} = 0.0254$

And we find the ex post paratemers: $\left\{\theta, \iota, e^{row}, \zeta, g\right\}$
By using the net-worth evolution, we can find $\iota$:

$$\iota = \frac{1 - \chi((r^G - R)lev + R}{lev}$$

Then, from the FOC of bankers, we can get the bank's discount factor:

$$\nu = \frac{1 - \chi}{1 - \chi\beta((r^G - R)lev + R)}$$

And from the leverage equation, we get the fraction of capital that can be diverted:

$$\theta = \frac{\nu}{lev} + \beta((r^G - R)\nu)$$

In the model, pollution is represented in arbitrary units. However, in order to align with real-world measurements, our aim is to calibrate the model so that the steady-state level of pollution corresponds to $x^{GtC}$ (gigatons of carbon). This choice of $x^{GtC}$ will result in a damage parameter, denoted as $\bar{D}$, that matches the estimate provided by Gibson and Heutel (2023). By achieving this calibration, we ensure that the model's pollution levels are more meaningful and relevant in the context of actual carbon emissions and their associated impacts.

$$\overline{D} = \overline{D}_0 + \overline{D_1} x^{GtC} + \overline{D_2} x^{GtC2}$$

Where $\overline{D_1}$ and $\overline{D_2}$ are proposed by Gibson and Heutel (2023). We need to find $D_1$ and $D_2$ in our model. We define the rest of the world emissions as: $e^{row} = RoW \times \bar{e}$, and from the pollution stock in steady-state ($\overline{x}$). Then we get:

$$D_1 = \overline{D_1} \frac{x^{Gtc}}{\overline{x}}$$

$$D_2 = \overline{D_2} \left( \frac{x^{Gtc}}{\overline{x}} \right)$$

## Appendix C: Banker's Problem Maximization

We solve this problem using the solution Ferrari and Nispi Landi (2024) proposed for this specific setting.

Let $t, t+i$ be the stochastic factor applying in period $t$ to earnings at $t+i$. Each banker exits the market with probability $(1-\chi)$ getting $NW_{t+1}$ at the beginning of period $t+i$. With probability $\chi$, a banker continues in this activity. Therefore the value of a bank is:

$$V_t^f = \max \; E_t \left[ \sum_{i=0} (1-\chi)\chi^i \beta^{i+1} M_{t,t+1} NW_{t+1+i} \right]$$

Subject to:

$$\frac{NW_t}{NW_{t-1}} = (r_t^G - r_t^B) lev_{t-1}^g + (r_t^B - \frac{r_{t-1}}{\pi_t}) lev_{t-1} + \frac{r_{t-1}}{\pi_t} - \frac{\kappa_F}{2} (\frac{lev_t^g}{l_{t-1}} - b^*)^2 \tag{33}$$

Recursively writing the expected terminal wealth:

$$\frac{V_t^f}{NW_t} = \max \; E_t \left[ (1-\chi) \; M_{t,t+1} \frac{NW_{t+1}}{NW_t} + \chi \beta M_{t,t+1} \frac{V_{t+1}^f}{NW_{t+1}} \right]$$

And following Gertler and Karadi (2011), financial intermediaries face the collateral constraint:

$$V_t^f(NW_t) \geq \theta b_t^f$$

$$\frac{V_t^f(NW_t)}{NW_t} \geq \theta lev_t$$

As the standard solution in this literature, we guess the solution:

$$\frac{V_t^f}{NW_t} = a_{gt} lev_t^g + a_{bt} lev_t + a_{ct} (\frac{lev_t^g}{lev_t} - b^*)^2 + a_{dt}$$

Being $a_{kt}$ with $k = a, g, c, d$ the coefficients to be determined.

Rewriting the bank problem as:

$$\max \left[ a_{gt} lev_t^g + a_{bt} lev_t + a_{ct} (\frac{lev_t^g}{lev_t} - b^*)^2 + a_{dt} \right] + (1 + \gamma_{Ft}) - \gamma_{Ft} \theta lev_t$$

With $\gamma_{Ft}$ being the Lagrange multiplier. The FOC are:

$$\left[ a_{gt} + \frac{2a_{ct}}{lev_t} (\frac{lev_t^g}{lev_t} - b^*) \right] (1 + \gamma_{Ft}) = 0$$

$$\left[ a_{bt} - \frac{2a_{ct} lev_t^g}{lev_t^2} (\frac{lev_t^g}{lev_t} - b^*) \right] (1 + \gamma_{Ft}) = \gamma_{Ft} \theta$$

Then, from the first FOC, we get the following:

$$a_{gt} = -\frac{2a_{ct}}{lev_t} (\frac{lev_t^g}{lev_t} - b^*)$$

We get the formula for $\gamma_{Ft}$ from the second condition. Then, using the guessed solution, we get:

$$\frac{V_t^f}{NW_t} = \max \; E_t \left[ (1 - \chi) \, M_{t,t+1} \frac{NW_{t+1}}{NW_t} + \chi \beta M_{t,t+1} \frac{V_{t+1}^f}{NW_{t+1}} \right]$$

$$\frac{V_t^f}{NW_t} = \max \; E_t \left[ (M_{t,t+1} \frac{NW_{t+1}}{NW_t} [(1 - \chi) + \chi \frac{V_{t+1}^f}{NW_{t+1}}] \right]$$

$$\frac{V_t^f}{NW_t} = \max \; E_t \left[ (M_{t,t+1} \nu_{t+1} \frac{NW_{t+1}}{NW_t} \right]$$

Where $\nu_t$ is the effective bank's SDF with $\nu_t = 1 - \chi + \chi \left[ a_{bt} - \frac{2a_{ct} lev_t^g}{lev_t^2} (\frac{lev_t^g}{lev_t} - b^*)^2 \right]$

Given the Banks' constraint by the evolution of net worth, we can find the remaining coefficients:

$$a_{gt} =_t \left[ M_{t,t+1} \nu_{t+1} (r_{t+1}^g - r_{t+1}^b) \right]$$

$$a_{bt} =_t \left[ M_{t,t+1} \nu_{t+1} (r^b_{t+1} - \frac{r_t}{\pi_{t+1}}) \right]$$

$$a_{ct} =_t \left[ M_{t,t+1} \nu_{t+1} \frac{r_t}{\pi_{t+1}} \right]$$

$$a_{dt} = -\frac{\kappa_F}{2}{}_t \left[ M_{t,t+1} \nu_{t+1} \right]$$

Using the first FOC, we get the following:

$$E_t M_{t,t+1}\, \nu_{t+1} \left( r_{g,t+1} - r_{b,t+1} - \left( \frac{lev_{g,t}}{lev_t} - b^* \right) \frac{\kappa_F}{lev_t} \right) = 0$$

Now, we can get the respective expression for the optimal leverage:

$$\theta lev_t = a_{gt} lev^g_t + a_{bt} lev_t + a_{ct} (\frac{lev^g_t}{lev_t} - b^*)^2 + a_{dt}$$

$$lev_t = \frac{M_{t,t+1}\, \nu_{t+1} \left( \frac{r_t}{\pi_{t+1}} + (r_{g,t+1} - r_{b,t+1})\, lev_{g,t} - \frac{\kappa_F}{2} \left( \frac{lev_{g,t}}{lev_t} - b^* \right)^2 \right)}{\theta - M_{t,t+1}\, \nu_{t+1} \left( r_{b,t+1} - \frac{r_t}{\pi_{t+1}} \right)}$$

Finally, using the previous conditions, we get the resulting formula for $\nu_t$:

$$\nu_t = 1 - \chi +, E_t M_{t,t+1}\, \nu_{t+1}\, \chi \left( \frac{r_t}{\pi_{t+1}} + (r_{g,t+1} - r_{b,t+1})\, lev_{g,t} + lev_t \left( r_{b,t+1} - \frac{r_t}{\pi_{t+1}} \right) - \frac{\kappa_F}{2} \left( \frac{lev_{g,t}}{lev_t} - b^* \right)^2 \right)$$